RECLAMATION

Managing Water in the West

Analysis and Design Recommendations of Rio Grande Width

Technical Service Center
Sedimentation and River Hydraulics Group

Technical Report No. SRH-2018-24

U.S. Department of the Interior
Bureau of Reclamation

September 2018

Mission Statements

The U.S. Department of the Interior protects America's natural resources and heritage, honors our cultures and tribal communities, and supplies the energy to power our future.

The mission of the Bureau of Reclamation is to manage, develop, and protect water and related resources in an environmentally and economically sound manner in the interest of the American public.

REPORT DOCUMENTATION PAGE

Form Approved
OMB No. 0704-0188

T1. REPORT DATE 09/2018	**T2. REPORT TYPE** Project	**T3. DATES COVERED** 10/1/2017 – 07/30/2018
T4. TITLE AND SUBTITLE Analysis and Design Recommendations of Rio Grande Width Technical Report No. SRH-2018-24		**5a. CONTRACT NUMBER** **5b. GRANT NUMBER** **5c. PROGRAM ELEMENT NUMBER**
6. AUTHOR(S) Blair Greimann and Nathan Holste		**5d. PROJECT NUMBER** **5e. TASK NUMBER** **5f. WORK UNIT NUMBER** 86-68240
7. PERFORMING ORGANIZATION NAME(S) AND ADDRESS(ES) Sedimentation and River Hydraulics Group Technical Service Center, Bureau of Reclamation, Denver, CO 80225		**8. PERFORMING ORGANIZATION REPORT NUMBER**
9. SPONSORING / MONITORING AGENCY NAME(S) AND ADDRESS(ES) Albuquerque Area Office U.S. Department of the Interior, Bureau of Reclamation, Albuquerque, NM		**10. SPONSOR/MONITOR'S ACRONYM(S)** **BOR/USBR:** Bureau of Reclamation DOI: Department of the Interior **11. SPONSOR/MONITOR'S REPORT NUMBER(S):** SRH-2018-24
12. DISTRIBUTION / AVAILABILITY STATEMENT Final report will be available by contacting Albuquerque Area Office		
13. SUPPLEMENTARY NOTES		
14. ABSTRACT *(Maximum 200 words)* .		
15. SUBJECT TERMS: River Width, Rio Grande, Geomorphology		

16. SECURITY CLASSIFICATION OF: U			**17. LIMITATION OF ABSTRACT**	**18. NUMBER OF PAGES**	**19a. NAME OF RESPONSIBLE PERSON:** Blair Greimann
a. REPORT U	**b. ABSTRACT** U	**c. THIS PAGE** U	**U**	20	**19b. TELEPHONE NUMBER** 303-445-2563

S Standard Form 298 (Rev. 8/98)
P Prescribed by ANSI Std. 239-18

PEER REVIEW DOCUMENTATION

Report Title: Analysis and Design Recommendations of Rio Grande Width

Client: Upper Colorado Region, Albuquerque Area Office

Technical Report No. SRH-2018-24

Prepared by:

BLAIR GREIMANN Digitally signed by BLAIR GREIMANN Date: 2018.09.28 08:55:37 -06'00'

_________________________________ Date:____________

Blair Greimann, Ph.D., P.E.
Hydraulic Engineer, Sedimentation and River Hydraulics Group (86-68240)

NATHAN HOLSTE Digitally signed by NATHAN HOLSTE Date: 2018.09.27 16:48:10 -06'00'

_________________________________ Date:____________

Nathan Holste, M.S., P.E.
Hydraulic Engineer, Sedimentation and River Hydraulics Group (86-68240)

Review Certification

Peer Reviewer: I have reviewed the assigned items/sections(s) noted for the above document and believe them to be in accordance with the project requirements, standards of the profession, and Reclamation policy.

DREW BAIRD Digitally signed by DREW BAIRD Date: 2018.09.28 09:28:26 -06'00'

_________________________________ Date:____________

Drew Baird, Ph.D., P.E.
Hydraulic Engineer, Sedimentation and River Hydraulics Group (86-68240)

JOEL SHOLTES Digitally signed by JOEL SHOLTES Date: 2018.09.28 08:44:04 -06'00'

_________________________________ Date:____________

Joel Sholtes, Ph.D., P.E.
Hydraulic Engineer, Sedimentation and River Hydraulics Group (86-68240)

Table of Contents

Page

Table of Figures

Page

Table of Tables

Acronyms and Abbreviations

1D	one dimension
Agg/Deg	Aggradation/Degradation cross section lines
ASCE	American Society of Civil Engineers
cfs	cubic feet per second
HEC-RAS	Hydrologic Engineering Center River Analysis System
Reclamation	Bureau of Reclamation
RM	river mile
TSC	Technical Service Center
USGS	U.S. Geological Survey
WY	water year

Citation:
Greimann, B. and Holste, N. (2018). Analysis and Design Recommendations of Rio Grande Width, Technical Report No. SRH-2018-24, Prepared for Albuquerque Area Office, Bureau of Reclamation, Albuquerque, NM.

Key Words: River Width, Sediment Transport, Middle Rio Grande

Acknowledgments

Dr. Ari Posner of the Albuquerque Area Office provided a database that included channel width, length, and bed material size. This data expanded on previous efforts by the Technical Service Center, led by Paula Makar, Jan Oliver, Dave Varyu, and others, to digitize planforms from aerial imagery and develop channel geometry. This work provided the foundation for analyses in the current study and is gratefully acknowledged.

1 Introduction

The Albuquerque Area Office (AAO) requested the Technical Service Center (TSC) develop channel width design recommendations that could be applied to channel-related project designs on the Middle Rio Grande, which extends from Cochiti Reservoir to Elephant Butte Reservoir.

A number of reports (e.g., Makar and AuBuchon, 2012; Scurlock, 1998; Lagasse, 1980) document the historical Middle Rio Grande conditions and the dramatic geomorphic changes that have occurred since the early 1900s. Geomorphic changes have been driven by events such as floods and drought, dam construction, vegetation clearing, operation of the low flow conveyance channel, and the construction of levees, channelization, and jetty jacks (see Figure 1 in Makar and AuBuchon, 2012). The integrated outcome of these events has been a trend of channel narrowing and vegetation encroachment, channel incision and bed material coarsening (primarily between Cochiti and Albuquerque) and an overall simplification of the channel geometry and planform as the river has become less dynamic. The channel width analysis presented in this report provides a tool for understanding the interrelated geomorphic parameters and for designing projects on the contemporary Middle Rio Grande.

To provide recommendations, first a regression analysis of the width component of the “downstream hydraulic geometry” is performed. This refers to the average width over some river distance and typically assumes “bankfull” dimensions where flow is just contained by the main channel before spilling out into the floodplain (ASCE, 2008). “Dominant discharge” or “channel-forming flow” are other terms that may approximate bankfull discharge (Doyle et al., 2007; Sholtes et al., 2016), which is the input flow implied by downstream hydraulic geometry equations. These equations describe the downstream variation in channel geometry parameters (top width, mean depth, mean velocity, slope, and friction) at a discharge of constant recurrence interval (Singh et al., 2003). Hydraulic geometry regression analysis can be used to understand how the flow, bed material, slope, vegetation cover, and bank height affect the channel width. It can also be used to estimate channel widths for design purposes. A limitation is that downstream hydraulic geometry analysis is an extension of regime theory and typically assumes a stable channel, or a channel in equilibrium (NRCS, 2007). The Middle Rio Grande, with its frequent changes in geomorphic drivers and corresponding channel adjustments, does not fit the classic definition of a stable channel. This required a slightly different analytical approach, as described later in this report.

Secondly, the width component of the “at-a-station” geometry is analyzed. This analysis defines the wetted top-width as a function of flow and other channel variables at a particular cross section. At-a-station data typically consists of more detailed measurements for a given location at a certain discharge and time period.

At-a-station geometry does not imply a bankfull or dominant discharge and includes a range of low to high flows.

Lastly, a design methodology is proposed in which the above information is used in the context of various restoration projects. Channel narrowing has been one of the most dominant geomorphic trends on the Middle Rio Grande over the last century (Posner, 2017; Baird, 2015; Makar and AuBuchon, 2012). In many reaches, incision and river bed lowering has been associated with channel narrowing. Possible applications of the proposed design methodology include vegetation clearing adjacent to the existing channel or determining an appropriate width for channel relocation projects.

2 Review of other Studies

A review of previous studies on predicting stream width is given in Baird (2015) and is not reproduced here. However, additional comment on the previous methods is necessary.

2.1 Middle Rio Grande Sediment Studies (Reclamation, 1961)

Reclamation (1961) developed an equation to estimate the cleared channel design widths for the MRG between Cochiti and the Rio Puerco. The channelization was limited to the undeveloped channel and floodplain (known collectively as the "floodway"), which was mostly between levees constructed by the Middle Rio Grande Conservancy District (MRGCD) during the 1930s. The goal was to develop a cleared channel within the existing floodway that would be consistent with the hydraulic and sediment transport requirements. Construction of the channel included clearing vegetation, placing permeable steel jetties, and excavating pilot channels through high points in the alignment.

The Reclamation 1961 equation was patterned after the unpublished Maddock equation, which determines the width of an alluvial river as a function of discharge, slope, roughness, sediment concentration, and sediment fall velocity (Reclamation, 1961). The USGS collaborated with Reclamation to obtain 301 measurements of hydraulic and sediment characteristics on the MRG between Cochiti and San Antonio during 1952–1957. Total load was calculated using the Modified Einstein Procedure (MEP). Statistical methods were used to derive an empirical regression equation from the dataset that would be applicable to the data collection reach. A summary of the data parameter ranges is presented below in Table 1. Two equations were derived by testing thirteen variables and finding that seven of the variables were statistically significant. One of the equations was for flow velocity and the other was for Manning's roughness. Figure 1 and Figure 2 demonstrate that the equations (Eq. 1 and Eq. 2 below) provide a reasonably accurate prediction of average depth and velocity.

Although the velocity and Manning's roughness equations perform relatively well, a multi-variable regression analysis using width as the dependent variable was never conducted. Instead, the velocity and roughness equations were combined using the continuity equation ($Q = VA$) and the simplified Manning's equation ($V = \frac{1.486}{n} d^{2/3} S^{1/2}$). Reclamation (1961) does not explain the specifics of how the four equations were combined to solve for width (Eq. 3 below). There appears to be circular reasoning in the derivation because the "observed" Manning's *n*-values were back-calculated using measured flow parameters and the Manning's equation. The Manning's equation was then applied a second time to substitute for the derived Manning's regression formula.

This substitution method produced a final width equation that contains interdependent terms. The velocity regression contains total sediment concentration (C_t) and the Manning's regression contains total sand concentration (C_{sn}). When these were combined in the width equation, C_{sn} is in the numerator and C_t is in the denominator, yet C_t is a function of C_{sn}. Similarly, the velocity regression contains fall velocity and the Manning's regression contains temperature. In the final width equation, temperature is in the numerator and fall velocity is in the denominator, yet fall velocity is a function of temperature. The 1961 width equation is most sensitive to slope (exponent of 3.184) a term that was not statistically significant in the velocity or roughness regressions prior to the Manning's equation substitution. Figure 3 demonstrates that the equation does not reliably predict channel width, even for the dataset it was derived from.

Additionally, the 1961 equation resulted in narrow channel widths when applied to a contemporary channel realignment design scenario on the Bosque del Apache National Wildlife Refuge. For the realignment project, the equation resulted in design widths of 130 ft, 170 ft, and 200 ft for discharges of 2000 cfs, 3000 cfs, and 4000 cfs, respectively. These design widths are all smaller than the current reach average active channel width of 250 – 300 ft. The 1961 width equation is not recommended for design based on the reasons discussed in this section.

Table 1. Range of parameters used to develop Reclamation (1961) width equation.

	Min	1st Quartile	Median	3rd Quartile	Max	Mean
Q (cfs)	17.6	348	612	1,340	6,440	1,129
V (ft/s)	0.63	1.81	2.21	2.85	7.36	2.53
n	0.0113	0.0227	0.0279	0.0329	0.0790	0.0283
d (ft)	0.42	1.18	1.43	1.76	5.57	1.60
W (ft)	26	130	207	275	665	220
D_{35} (mm)	0.11	0.22	0.26	0.30	0.95	0.27
C_t (ppm)	30.6	1,300	2,430	4,810	134,760	6,119
C_{sn} (ppm)	1.52	557	1,230	2,260	22,420	1,803
V_t (ft/s)	0.000267	0.0206	0.0410	0.0673	0.16100	0.0467
T (°F)	32	56	65	72	85	63
S (ft/ft)	0.000588	0.00086	0.00110	0.00129	0.00150	0.00109

$$V = 0.6385 d^{0.485} w^{0.0306} {C_t}^{0.170} {V_t}^{0.112} \tag{1}$$

$$n = 0.5295 {D_{35}}^{0.163} {C_{sn}}^{-0.156} T^{-0.184} \tag{2}$$

$$W = \frac{17{,}470 * Q^{0.778} S^{3.184} {C_{sn}}^{0.992} T^{1.171}}{{C_t}^{1.214} {V_t}^{0.800} {D_{35}}^{1.035}} \tag{3}$$

where:

V = mean velocity of water (ft/s),
n = Manning's roughness coefficient,
d = mean depth of cross section (ft),
W = width of water surface (ft),
C_t = total sediment concentration (ppm),
V_t = mean settling velocity of the total sediment (ft/s),
D_{35} = size of the bed material that 35% is finer than (ft),
C_{sn} = total sand concentration (ppm), and
T = temperature of water (°F)

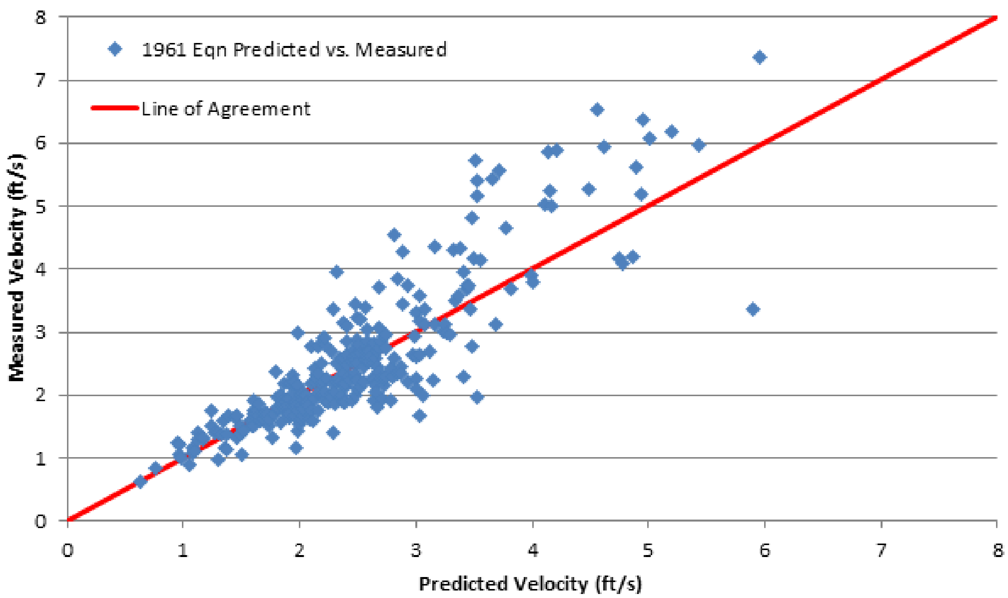

Figure 1. Comparison of measured vs. predicted velocity for Reclamation (1961) data.

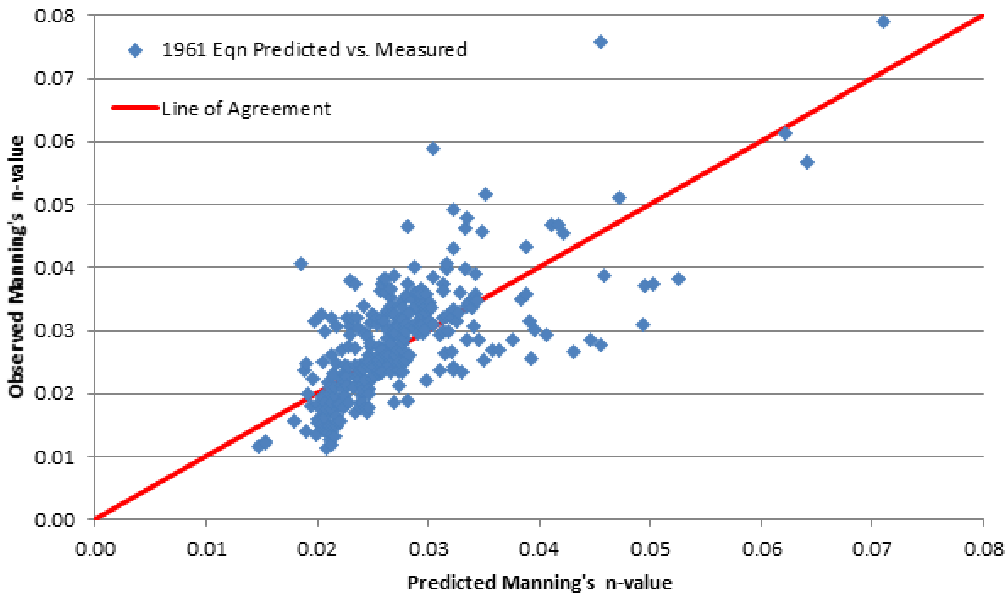

Figure 2. Comparison of measured vs. predicted Manning's roughness for Reclamation (1961) data.

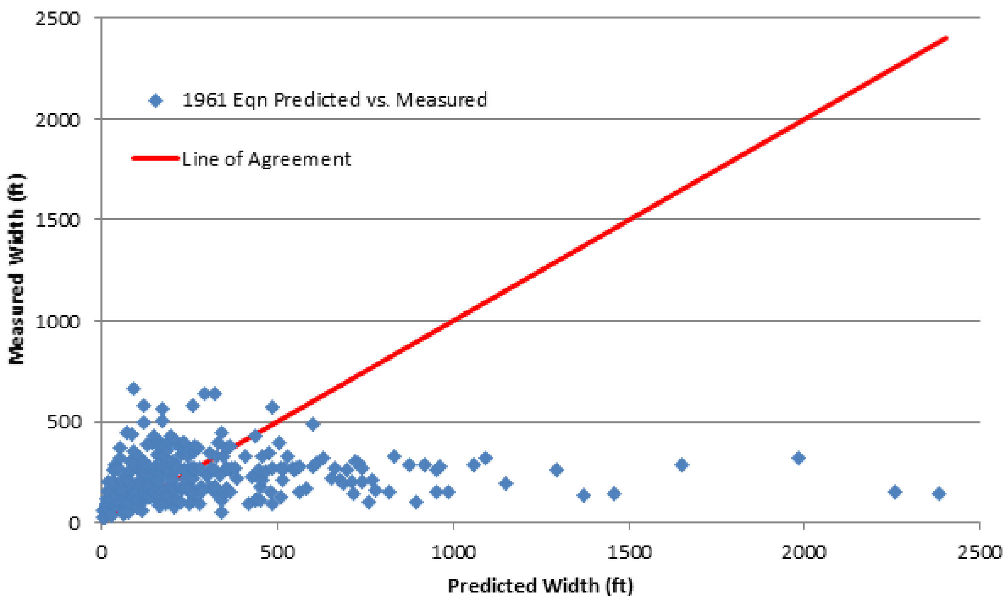

Figure 3. Comparison of measured vs. predicted channel width for Reclamation (1961) data.

2.2 Stable Channel Analysis

There is a long history of analyzing stable channel width as a function of flow, bed material and slope (Julien, 2002) and equations are usually of the form:

$$W = aQ^b D50^c S^d \quad (4)$$

Julien (2002) suggests that a = 1.33, $b = 0.44$, $c = -0.1$, and $d = -0.2$ which is in general agreement with other literature on alluvial channels (Parker et al., 2007). This equation assumes Q is in m^3/s, *D50* is in m, and *S* is non-dimensional.

NRCS (2007) suggested the following design equation for channel width:

$$W = aQ^{0.5} \quad (5)$$

where a was a function of tree cover: a = 2.86 for less than 50% tree cover and a = 1.83 for more than 50% tree cover.

In contrast to the negative exponent on slope in the above equation, Leon et al. (2009) found a positive correlation between slope and width between San Acacia and San Marcial on the Rio Grande and explained the positive correlation of *W* and *S* by using stable channel analysis saying the wider, steeper reach is necessary to transport the same sediment as the narrower, flatter reach. For channel conditions that are wider than the width at minimum slope, they predict that the following relationship should exist between slope and width for two channel reaches (all other variables being equal):

$$W_1/W_2 = (S_1/S_2)^7 \quad (6)$$

One can see that width could be very sensitive to slope change as the power in the relationship is 7.

To further analyze the relationship between width and slope, additional simulations using a stable channel analysis program developed in the Sedimentation and River Hydraulics Group were performed in this study to further understand the implications. The program is similar to SAM Hydraulic Design Package for Channels (USACE, 1998). Simulations were performed assuming typical values observed on the Rio Grande but are not necessarily exactly representative of any particular location. These were performed to hopefully be instructive as to the types of geomorphic change occurring along the Rio Grande. The stable channel analysis is performed assuming a *D50* of 0.35 mm, which is typical of the reach around San Antonio Bridge. The input discharge is 5000 cfs, which was typical of the annual maximum of the daily average flows prior to 2002 (Figure 10). The Engelund-Hansen sediment transport formula is used, and the assumed Manning's roughness coefficient is 0.02 for the bed and 0.04 for the banks. These roughness values are representative of calibrated values from several previous hydraulic and sediment modeling studies on the Middle Rio Grande. The floodplain roughness and topography are not accounted for in the program; the method is only intended to represent main channel hydraulics and sediment transport. An effective channel side slope of 5H:1V is initially assumed. This is not necessarily equal to the physical side slope of the banks because the method assumes a trapezoidal channel shape, which only approximates the natural channel shape. A range of sediment bed material load concentrations is used, and a family of Width versus Slope curves is generated in Figure 4.

On the Rio Grande, the sediment loads have decreased since the construction of Cochiti Dam (Makar and AuBuchon, 2012), which has caused incision in many reaches, decreasing channel slope (Figure 12). The incision and decrease in channel slope then has then caused a decrease in channel width. The direction of this change is shown in Figure 4. The stable channel analysis methodology does not directly consider the effects that vegetation has on the channel form and assumes that vegetation will not limit bank erosion. Once narrowing has occurred, vegetation could encroach on the channel and prevent erosion if flows increase again.

The effect of decreasing flow is shown in Figure 5. The stable channel analysis describes the general trend that decreasing flow has on the channel width. The arrow shown on the figure demonstrates that if the slope and sediment concentrations stay the same, the stable width will decrease by almost a factor of 2.

The effect of changing channel side slope to 3H:1V instead of 5H:1V is shown in Figure 6. Decreasing the side slopes to 3H:1V increases the channel width for the same slope. As mentioned above it is difficult to exactly measure the side slope because the methodology assumes a trapezoidal shape that does not exactly represent the more complex channel shape.

The resulting channel depths of the analysis are given in Figure 7. Notice that for channel widths of more than 400 ft, the stable channel depth is less than 3 ft.

The stable channel analysis methodology can be useful to describing the direction of change expected when flow, bed material, and slope are changed. It may be difficult to use it to predict the channel width and slope in an absolute sense because the input variables and the sediment transport formulas have significant error associated with them that then propagates into the error of the predicted width.

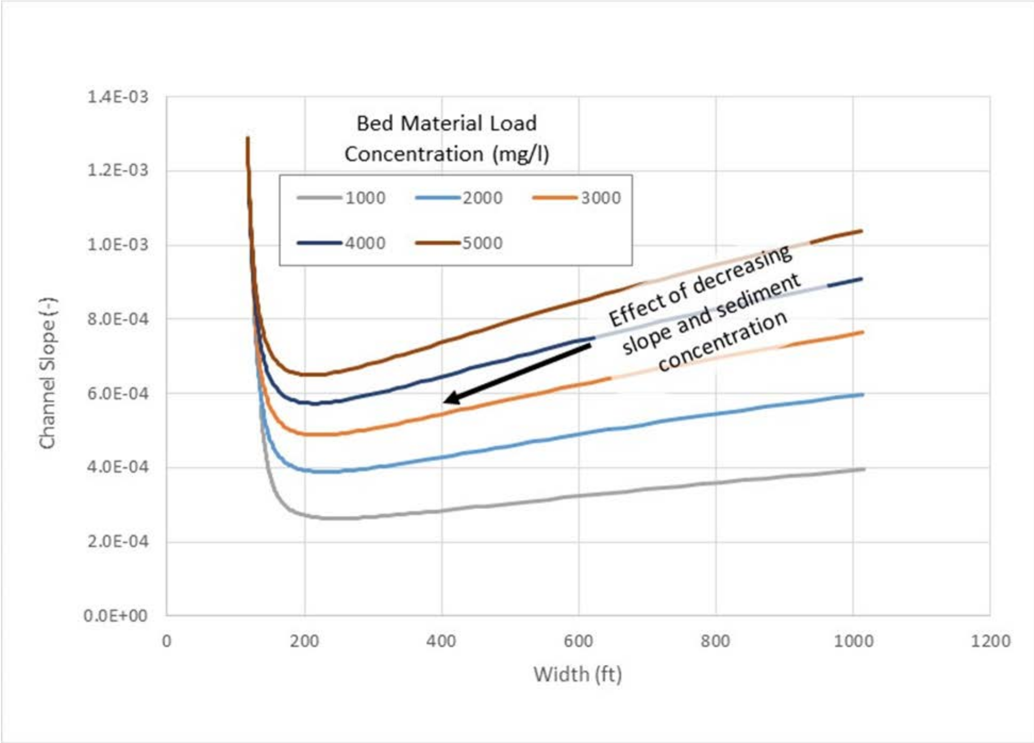

Figure 4. Various width versus slope curves for D50 = 0.35 mm and a range of potential bed material load concentrations.

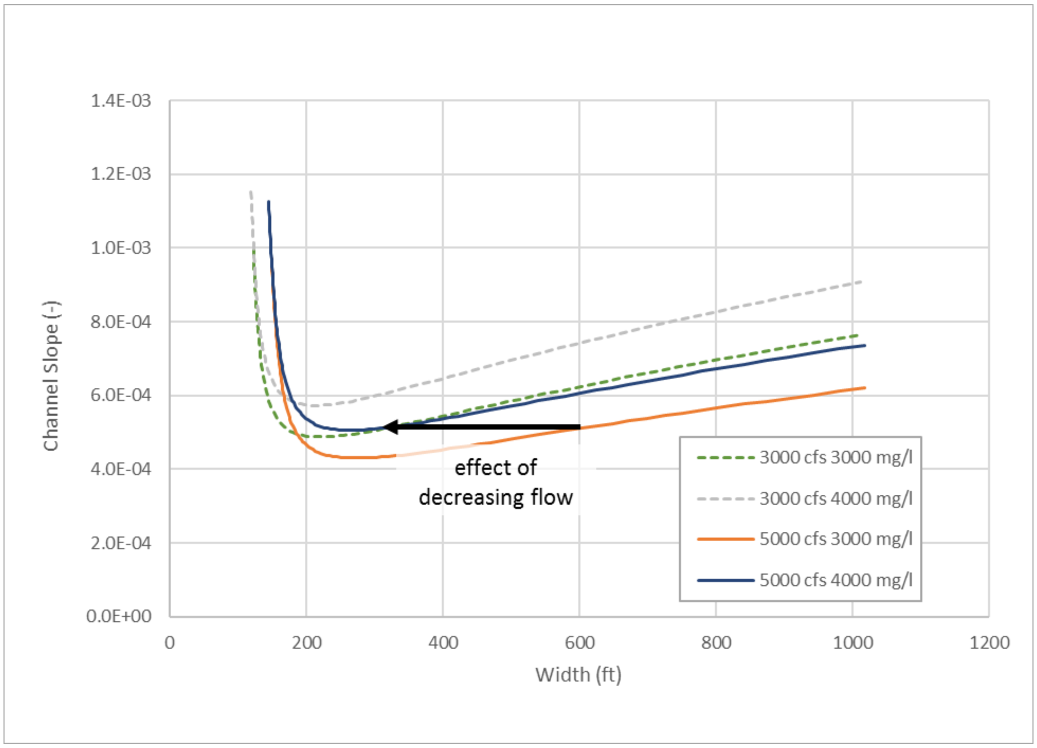

Figure 5. Various width versus slope curves for D50 = 0.35 mm and a range of potential bed material load concentrations and flow regimes.

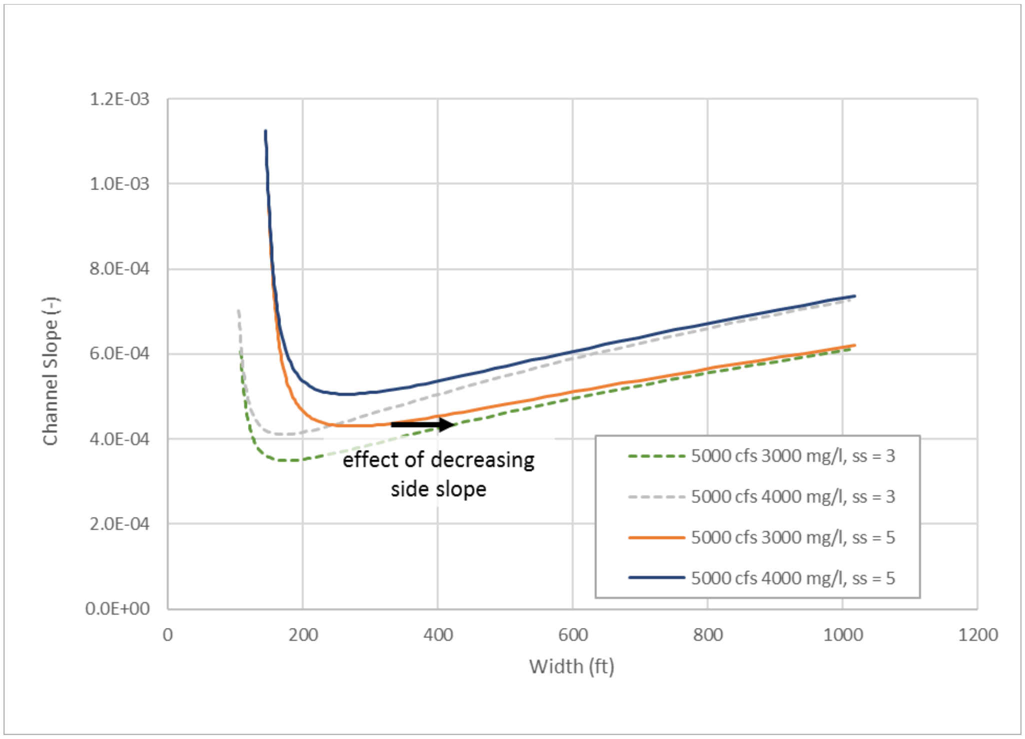

Figure 6. Various width versus slope curves for D50 = 0.35 mm and a range of potential bed material load concentrations and channel side slopes.

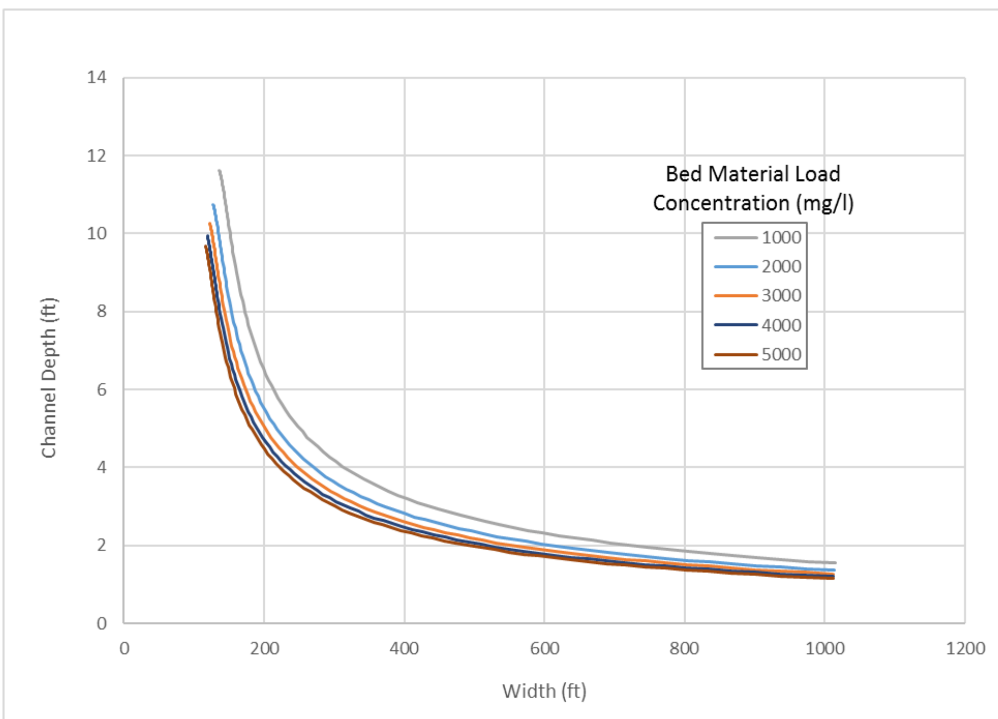

Figure 7. Various channel depth versus slope curves for D50 = 0.35 mm and a range of potential bed material load concentrations.

3 Downstream Geometry

The limitations of using existing methods for analysis and design of channel width on the Middle Rio Grande indicates the need for developing an improved downstream hydraulic geometry equation. The goal of the new equation is to better represent data on the Middle Rio Grande and how the river dynamically responds to changing flow, sediment loads, and other geomorphic drivers.

3.1 Definition of Middle Rio Grande Reaches

The downstream geometry is defined over a river reach and not at a specific cross section, therefore it is necessary to subdivide the Middle Rio Grande into reaches that have similar geomorphic characteristics. The reaches used in this study were generally consistent with the reaches defined in Posner (2017) as given in Figure 8, but some of the larger reaches were further subdivided based upon distinct changes within the reach. This is necessary because each reach at a given time period is essentially one data point to formulate the regression equation, and some reaches much longer than other reaches underweights data from that particular section of river. The Angostura reach was divided into two reaches by the AMAFCA North Diversion Channel outfall in northern Albuquerque, because this reach was substantially longer than others. The Isleta reach was divided into two reaches by the Burlington Northern and Santa Fe Railroad Bridge to shorten the length. The San Acacia Reach was divided by the confluence with Arroyo Alamillo because of a change in bank height: the reach from San Acacia to Arroyo Alamillo is substantially more incised than downstream of Alamillo. The River Mile 78 reach was divided into two reaches by Mesa Contadero because this geologic feature acts as a significant control on the river.

The final reach definition used in this study is given in Table 2. Reach lengths ranged from 4.1 to 24.9 miles and average 13.9 miles. Agg/Deg lines start at Line #17 near the USGS Cochiti Gage and progress downstream to Line #1962 at the "Narrows" within the Elephant Butte Reservoir Pool. The lines are nominally spaced 500 ft apart. Posner (2017) created polygons to represent the area between Agg/Deg lines to facilitate more consistent analysis. River Miles (RM) begin at RM 0 at Caballo Dam and progress upstream to RM 232.6 at Cochiti Dam. River miles at significant locations such as dams and bridges remain consistent, while river mile stations at intermediate locations are adjusted approximately every 10 years based on changes to channel length. 2002 RMs are used in this report to be consistent with previous reports. Reach 12 (Mesa Contadero to Full Pool) was not used in the regression analysis because it has been extensively channelized, has cohesive banks, and is significantly influenced by the pool elevation of Elephant Butte Reservoir. Appendix A documents the location and rationale of specific Agg/Deg locations that were also eliminated from the analysis.

Table 2. Reach Definition for Downstream Geometry.

Reach ID	Description	US Agg/Deg	DS Agg/Deg	US RM (2002)	Length (mi)
1	Cochiti to Angostura Diversion	19	236	232.6	22.5
2	Angostura Diversion to North Diversion Channel outfall	237	397	210.1	15.9
3	North Diversion Channel outfall to Isleta Diversion	398	656	194.2	24.9
4	Isleta Diversion to Agg/Deg 877	657	876	169.3	21.6
5	Agg/Deg 877 to Rio Puerco	877	1097	147.7	21.1
6	Rio Puerco to San Acacia	1098	1206	126.6	10.4
7	San Acacia to Arroyo Alamillo	1207	1246	116.2	4.2
8	Arroyo Alamillo to Arroyo de las Canas	1247	1398	112	16.9
9	Arroyo de las Canas to San Antonio Bridge	1399	1476	95.1	8.0
10	San Antonio Bridge to RM 78	1477	1585	87.1	9.0
11	RM 78 to Mesa Contadero	1586	1682	78.1	8.0
12	Mesa Contadero to Full Pool	1683	1724	70.1	4.1

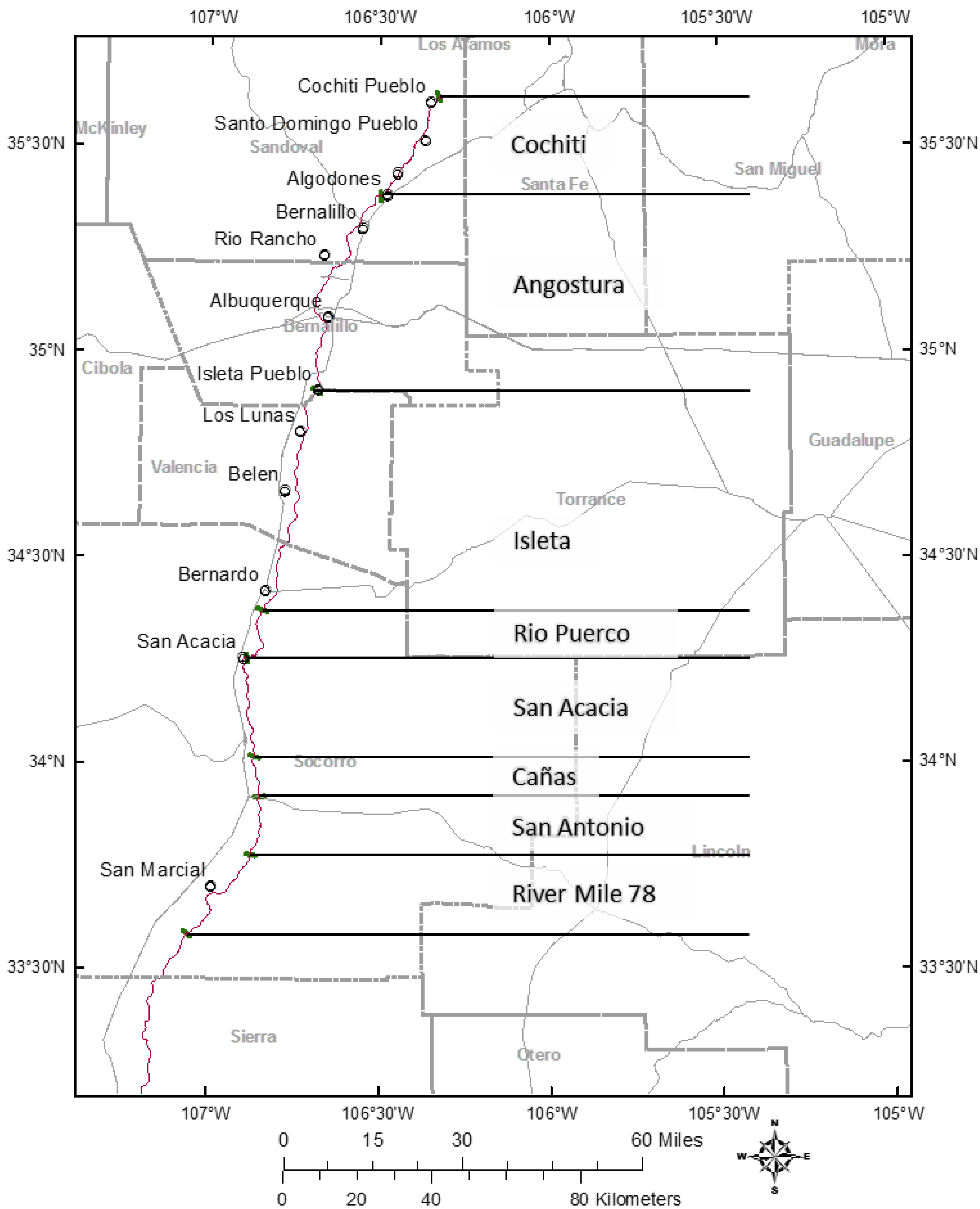

Figure 8. Rio Grande reaches defined in Posner (2017). The reaches Angostura, Isleta, San Acacia, and River Mile 78 are each divided into two reaches for this study.

3.2 Data

To conduct the downstream hydraulic geometry regression analysis, we compiled data on pertinent geomorphic and hydrologic variables along each reach over a number of decades. In this section, we describe the types of data we used in our analysis and the methods and sources we used to collect these. For each reach, the following data was obtained for the years 1962, 1972, 1992, 2002, and 2012:

1. A representative flow for the reach obtained from daily average stream flow records at USGS gages
2. Stream Width as defined by unvegetated channel width and/or bank lines delineated using aerial photography
3. Stream Bed Slope
4. Stream Bank Height
5. Stream Bed Material
6. Vegetation presence along stream bank

The final compiled dataset consisted of 11 reaches for each of the five years (1962, 1972, 1992, 2002, and 2012), thereby resulting in 55 data points available for width regression analysis. The six parameters listed above were obtained for each of the 55 combinations of reach and year.

3.2.1 Stream Flow

A unique assumption in this analysis is that stream width is not a constant in time, but rather responds to changing flow conditions. There is not a single, stable 2-yr flood value that is assumed to persist into the future. Nor is there then a “stable width” that persists into the future.

To demonstrate the long-term (decadal) cycles that can occur on the Rio Grande, a plot of the 8-year moving average of stream flow at each of the gages is given in Figure 9. The figure demonstrates that the Rio Grande has experienced long term cycles of wet and dry periods in the recent past. The channel has been narrowing since 1990 and some of this narrowing has been due to the dry conditions in the watershed and low flows in the river.

Several representative stream flows averaged over different periods of time were used to correlate with stream width. The three analyzed here are the 1) average of the annual maximum daily average, 2) maximum of the annual maximum daily average, and 3) average of the annual instantaneous peak flow. The average of the instantaneous peak flows would correspond to the 2.33-yr return period flood for the given time period. The coefficient of determination (R^2) of the linear regression equation between the logarithm of these three representative flows and the logarithm of the stream width was computed for different averaging periods ranging from 7 to 12 years (Table 4). The representative flow that gave the highest coefficient of determination was the average over the previous 8 years of the annual maximum of the daily average and this was the flow used to perform the regressions. The representative flows used in the study are given in Figure 10.

Table 3. Stream gages used in analysis.

USGS ID#	Name	Water Years of Operation	Years	River Mile (2002)
08313000	Otowi Bridge	1895-2017	122	257.5
08317400	Rio Grande Below Cochiti Dam	1971-2017	46	232.5
08319000	Rio Grande at San Felipe	1927-2017	90	216.5
08330000 & 08329500*	Rio Grande at Albuquerque	1942-2017	75	183.5
08354900 & 08355000**	Rio Grande Floodway at San Acacia	1936-2017	81	116
08358400 & 08358500***	Rio Grande Floodway at San Marcial	1900-2017	117	68.5

*08329500 gage is used prior to WY1992
**08355000 gage is used prior to WY1958
***08358500 gage is used prior to WY1950

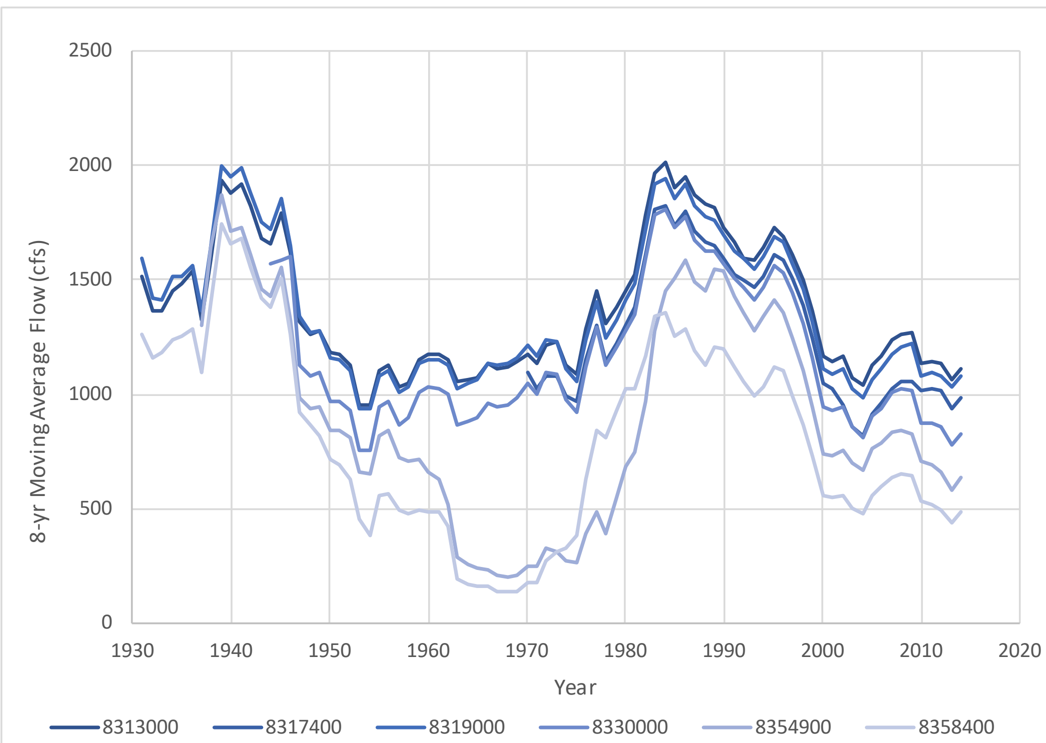

Figure 9. Eight-year moving average of annual average flow on the Middle Rio Grande at various stream gages as listed in Table 2, ordered upstream to downstream.

Table 4. The coefficient of determination of the relationship between representative stream flows and stream width.

Years	Coefficient of Determination of the Relationship between Representative Flow and Stream Width		
	Average of Annual Maximum over period	Maximum daily flow over period	Average of Annual Peaks
7	0.31	0.17	0.13
8	0.55	0.38	0.18
9	0.54	0.41	0.2
10	0.46	0.42	0.18
11	0.51	0.42	0.20
12	0.48	0.43	0.16

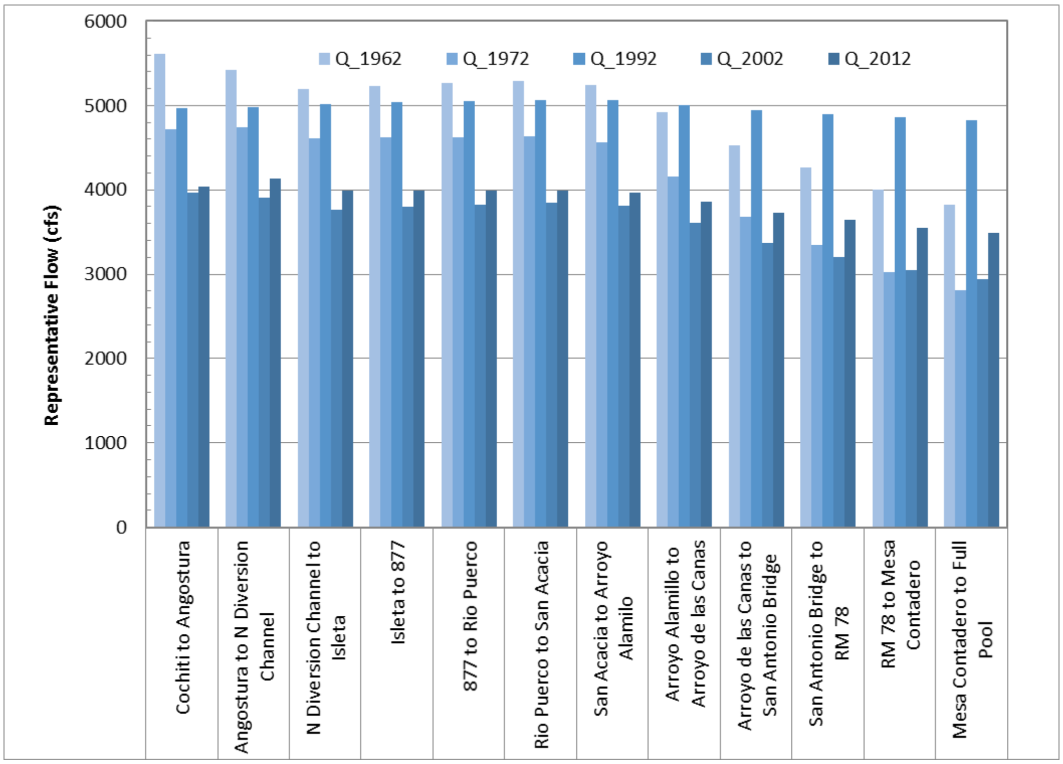

Figure 10. Representative Flows for each reach. The representative flow is the 8-year average of the annual maximum daily average flow.

3.2.2 Stream Width

The bankfull width was defined by digitizing the unvegetated width as defined by aerial photography for each of the years in the analysis (1962, 1972, 1992, 2002, and 2012). Efforts were made to distinguish alluvial channel width from floodplain areas that had been actively cleared. Delineating channel boundaries using remotely-sensed data results in uncertainty linked to image resolution, image rectification, and operator judgement. Posner (2017) then used these polygons to represent the section between consecutive Agg/Deg lines, which are spaced approximately 500 ft apart. Active channel width for a given Agg/Deg line was then calculated as the channel polygon area divided by the centerline length. The average width in each reach at each time period is given in Figure 11.

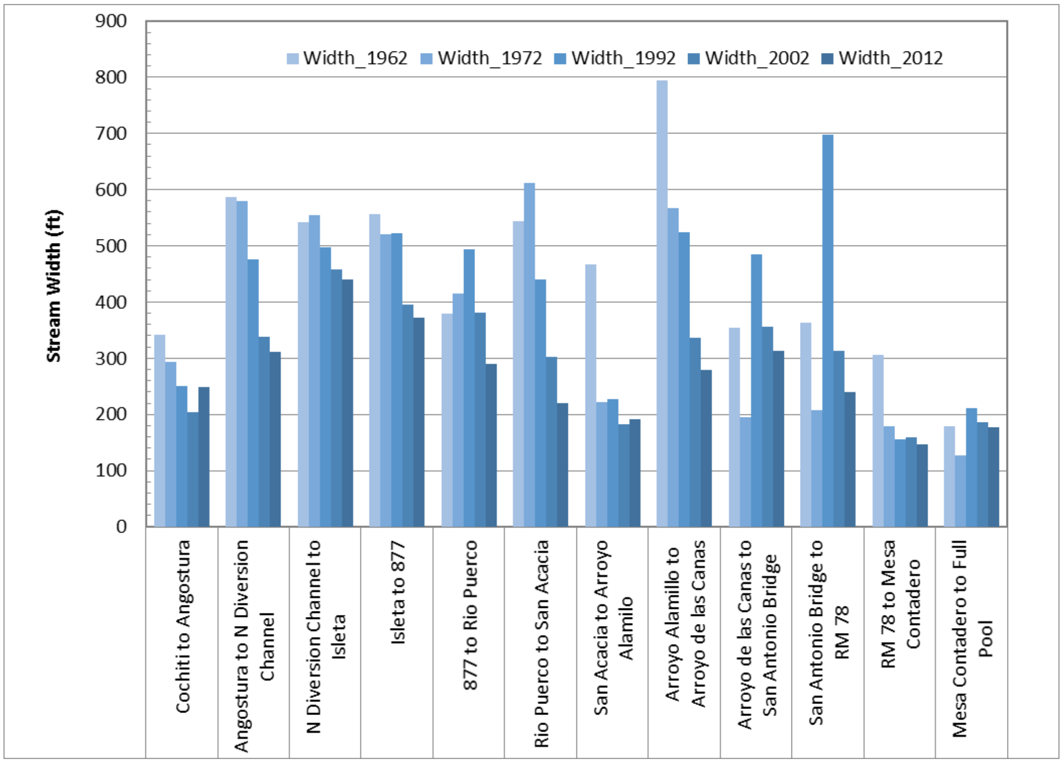

Figure 11. Reach Averaged Width in Middle Rio Grande.

3.2.3 Stream Bed Slope

The reach averaged stream bed slope was computed by differencing the bed elevation from the upstream end of the reach with the downstream end of the reach and dividing by the length of the reach. The bed elevations were taken from the HEC-RAS models of the reach for each of the years (1962, 1972, 1992, 2002 and 2012). The HEC-RAS models were derived from LiDAR or photogrammetry surveys of the river channel and the underwater portion of the channel was calculated based upon the observed water surface elevation and flow at the time of the survey (e.g., Varyu, 2013; Holmquist-Johnson and Makar, 2006). Therefore, the bed elevation used in this analysis is an average bed elevation in the low flow portion of the channel.

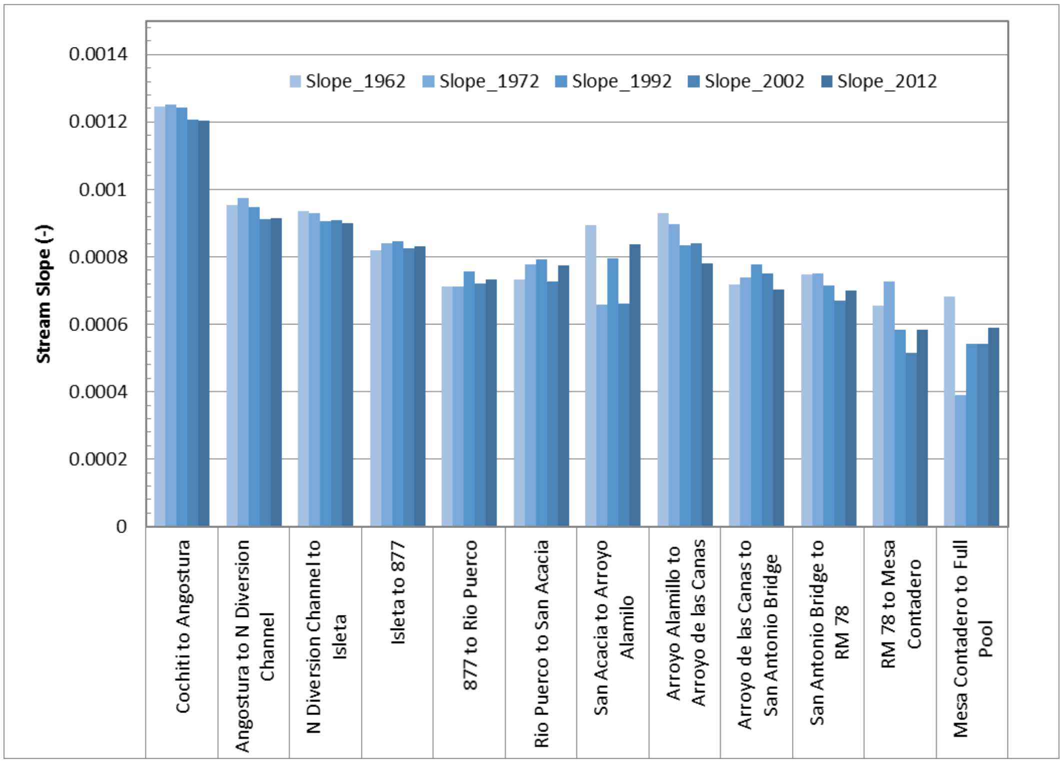

Figure 12. Reach Averaged Stream Slope.

3.2.4 Bank Height

The bank height was computed by taking the average of the left and right banks as defined in the HEC-RAS cross-sections of each reach (e.g., Varyu, 2013; Holmquist-Johnson and Makar, 2006) and differencing it with the minimum bed elevation. The minimum bed elevation in the HEC-RAS model is actually the average bed elevation at low flow because the HEC-RAS model was developed from photogrammetry performed at low flow that did not have below water information. The average bed elevation was computed by adjusting the bed of the cross section until the low flow water surface elevation matched the measured water surface elevations, assuming normal flow conditions. The reach averaged bank height is shown in Figure 13.

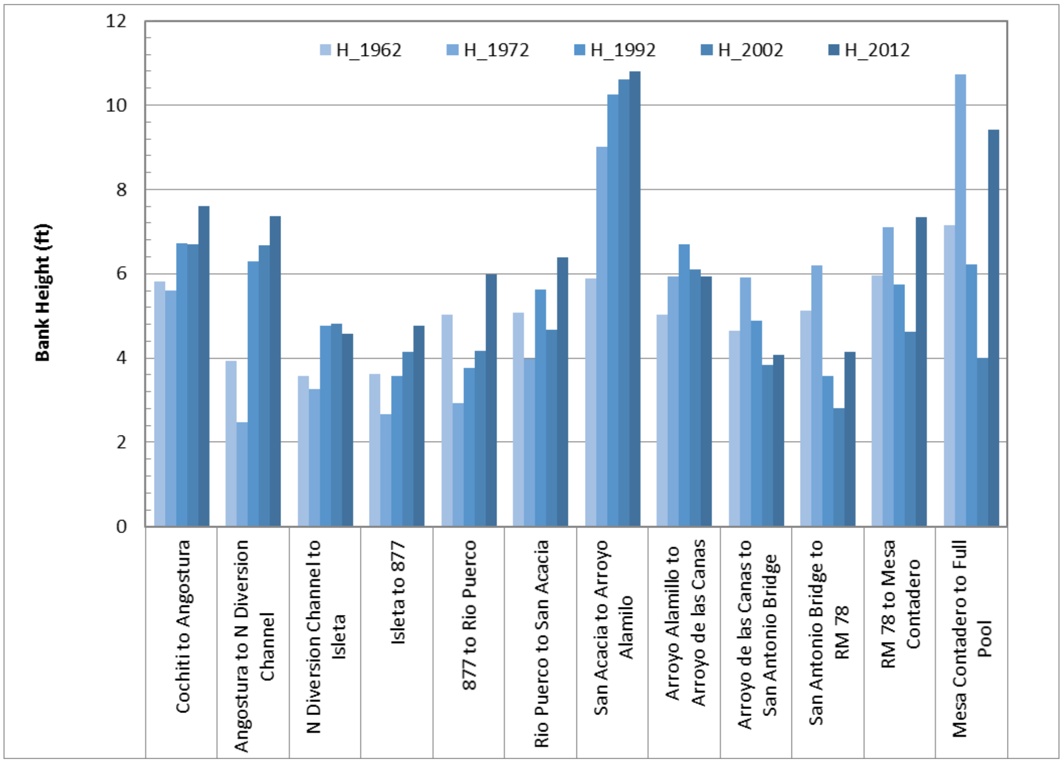

Figure 13. Reach averaged bank height.

3.2.5 Bed Material

The bed material used for the downstream geometry analysis consisted of measurements taken between 1952 and 2015. There have been several studies and sampling programs measuring bed material on the MRG. Reclamation and USGS collaborated on a data collection effort during the 1950s, which resulted in 301 measurements between 1952 and 1957 at a range of locations from Cochiti to San Antonio. A Reclamation report (Reclamation, 1961) contains a summary table of the measurements, while a series of USGS professional papers provide additional details and analyses (Culbertson and Dawdy, 1964; Nordin and Beverage, 1965; Nordin, 1964).

There were no reported bed material measurements available that were sampled between 1962 and 1972 and therefore, the bed material in 1972 was assumed to be similar to that in 1962. Cochiti Dam closed in 1974 and we assumed pre-dam data would be more representative of stream conditions in 1972 then post dam data.

The AAO has compiled a database with bed material data collected between 1970 and 2008, which was provided by Ari Posner (pers. comm., 2017). This database is a compilation of measurements made by Reclamation (AAO and TSC) and contractors (e.g., FLO Engineering, 1995). Most of the bed material data used in this study was obtained from the AAO database, with the addition of a few post-2008 samples collected by Reclamation and consultants. Bed material data show a marked increase in median grain size over the study period.

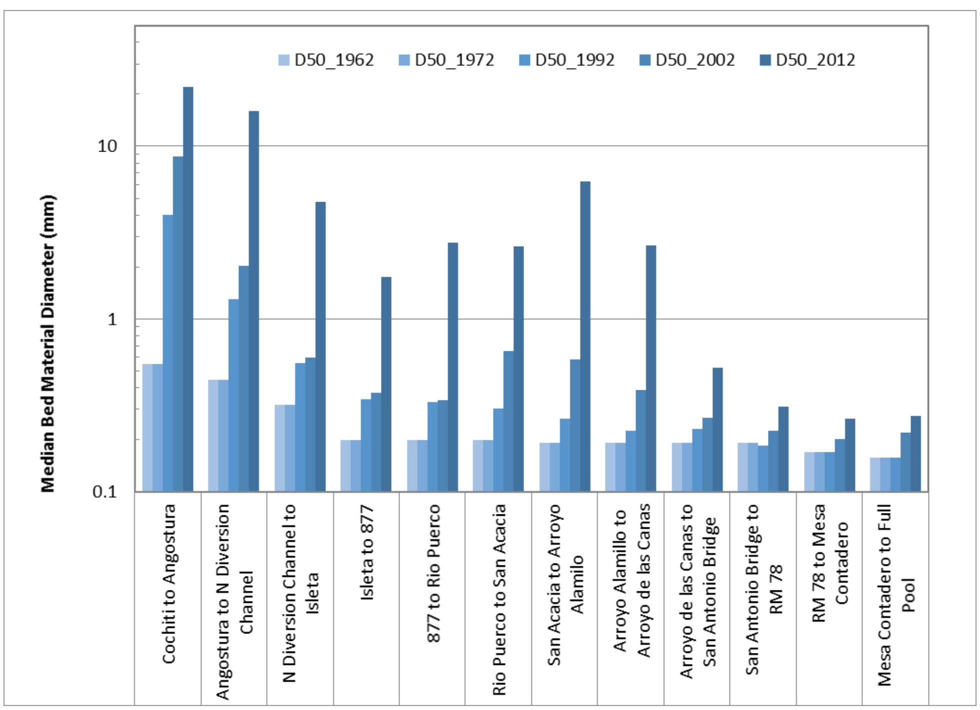

Figure 14. Reach averaged median bed material diameter (D50).

3.2.6 Fraction of Bank that is Vegetated

The fraction of the bank that is vegetated was computed by using aerial photography to assign a presence or absence of vegetation along the left and right banks at each Agg/Deg line for each time period. Vegetation coverage was delineated using the same polygons that were developed by Posner (2017) to determine channel width and length for each Agg/Deg line. Polygons were classified using a binary system of either “vegetated” or “non-vegetated”. Vegetated sections were defined as having bankline vegetation along 50 percent or more of the bank. Non-vegetated sections were defined as having bankline vegetation along less than 50 percent of the bank. The 50 percent criterion was selected to be consistent with NRCS (2007) and other alluvial channel hydraulic geometry studies. This represents the bank resistance to erosion, or the ability of the channel to widen during high flow events. Lateral constraints such as geologic features, revetted banks (e.g., riprap, jetty jacks), and levee roads were categorized as vegetated.

The percentage of bankline vegetation was then calculated for each reach during each available year. This percentage was calculated by dividing the number of vegetated Agg/Deg polygons within a reach by the total number of polygons, because each polygon represents the same nominal channel distance of 500 ft. For example, in 1962 the Angostura Reach had 94 vegetated Agg/Deg polygons out of 161 total polygons, resulting in a vegetation percentage of 58%. The representative vegetation fraction that is used in the analysis is the average vegetation coverage digitized from that year and the previous available year.

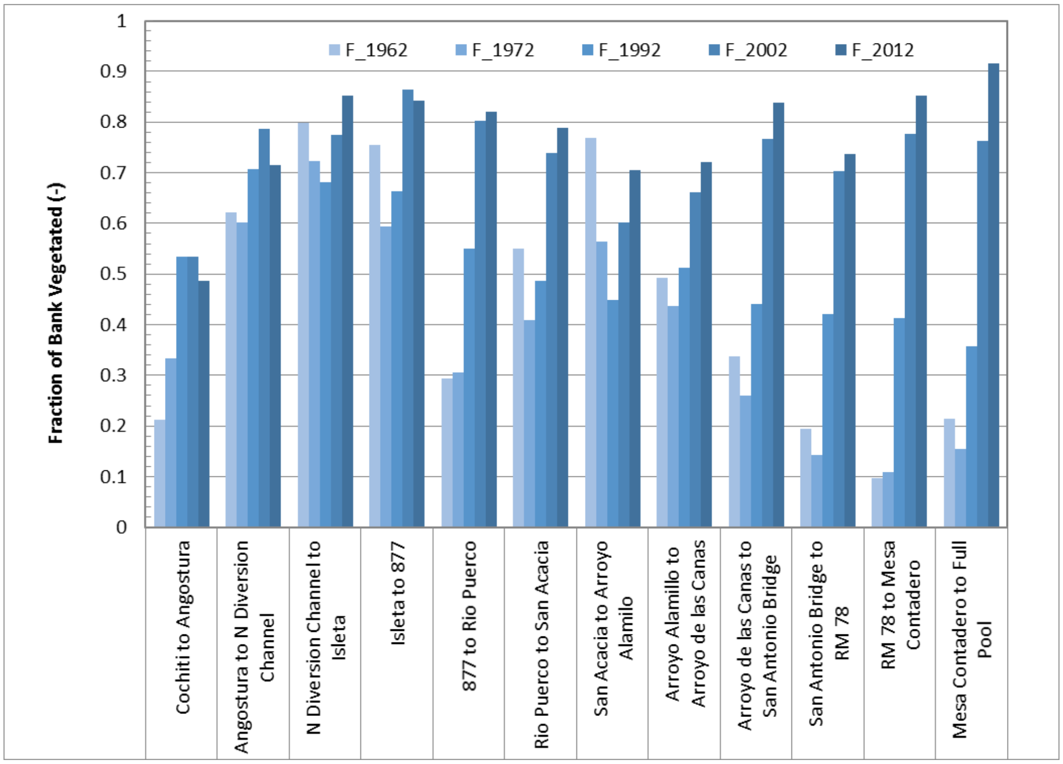

Figure 15. Fraction of stream bank that is vegetated.

3.3 Regression Analysis

In this analysis, multiple linear regression of the log-transformed variables is used to analyze the relationship between the reach average properties and stream width. Previous hydraulic geometry relationships have assumed channel width will eventually be static in time whereas this analysis assumes that the width is only a function of the flow and stream variables averaged over a period of a decade or less. This is consistent with the rather rapid response of the stream to changes in flow and sediment variables. It also recognizes the fact that the stream will likely continue to evolve to changing flow and sediment regimes imposed on it. Therefore, this analysis is not intended to be a "stable channel" analysis, but rather simply an analysis of the effect of various inputs on stream width.

The log transformed regression equation used in this analysis can be written as:

$$\ln W = \ln a' + b \ln S + c \ln D50 + d \ln Q + e \ln H + f\, F \qquad (7)$$

where W = stream width (ft)

S = stream bed slope (-)

$D50$ = stream median bed material diameter (mm)

Q = representative flow (cfs)

H = bank height (ft)

F = fraction of bank vegetated
a', b, c, d, e, f = constants in the regression equation

The constant a' needs to be bias corrected because the log transformation can bias the results in real space. In the equation used in practice, the coefficient a' needs to be replaced by a, where a is the bias corrected coefficient using the method proposed by Duan (1983), who used the smearing estimator to correct non-normality in the distribution of regression residuals. Duan's smearing estimator is based on the following equation,

$$a = a' \sum_{i=1}^{n} \exp(e)_i / n \tag{8}$$

where,

a' = biased regression coefficient
e_i = residuals from least squares regression (differences in natural logarithms of measured and computed suspended sediment concentration or bed load)
n = number of residuals used in linear regression.

Before performing the regression analysis, it is useful to understand the correlation matrix between the variables (Table 5). One can see that slope is highly correlated to $D50$ as would be expected because steeper streams typically have larger bed material. However, one also sees that slope is positively correlated to the representative flow, which is not typical. There is no causal link between flow and slope for the MRG over the study area, but flow losses due to diversion and infiltration are larger than the flow accumulations as one goes downstream and the slope decreases. Therefore, this is most likely only a correlative link. Another important factor is that bank height and $D50$ are positively correlated. This is likely because streams below large dams typically incise and become coarser due to the reduction in sediment bed material load. Some other important factors to be considered are that there is a positive correlation between width and slope, whereas it is usually assumed that there is a negative correlation between width and slope (Julien, 2002). On the Rio Grande, the positive correlation is likely because of two factors: 1) the flow decreases in the downstream direction whereas in most rivers the discharge increases in the downstream direction, and 2) because of the relatively high sediment loads, a wider channel may require a steeper slope to transport the sediment load (Leon et al., 2009).

Table 5. Correlation coefficient between regression variables

	Log W	*Log S*	*Log D50*	*Log Q*	*Log H*	*F*
Log W	-	0.31	-0.24	0.59	-0.60	0.08
Log S	0.31	-	0.51	0.39	0.05	-0.02
Log D50	-0.24	0.51	-	-0.14	0.37	0.36
Log Q	0.59	0.39	-0.14	-	-0.13	-0.17
Log H	-0.60	0.05	0.37	-0.13	-	-0.15
F	0.08	-0.02	0.36	-0.17	-0.15	-

If two independent variables are strongly correlated, then it is likely not necessary to include both variables. In fact, if both variables are included, the final regression model may have a worse predictive capability than a regression model that only includes one of the variables. This is generally termed the problem of collinearity.

To evaluate the problem of collinearity and to determine the best set of independent variables to use the regression analysis of various groups of variables is presented below and a comparison between the various models is given. We start with a model that incorporates all of the independent variables we evaluated for this study and then systematically reduce the variables in the model based on the values and significance levels of the coefficients associated with each variable. The multiple regression analysis was carried out in R© version 3.5.0 using the *lm* function in the stats v3.5.0 package and Excel 2016® using the Regression Tool. For all the analysis shown in this report, the two methods gave identical results. Linear modelling is supported by our log-transformed variables as the residuals of each model are generally not heteroschedastic and follow a normal distribution. Diagnostic plots and information demonstrating this are provided for each model in Appendix C.

To estimate the relative error between the predicted and measured widths and compare the accuracy of the multiple regression equations we evaluated, we used the following definition of the standard error:

$$\text{standard error} = \sqrt{\frac{\sum_{i=1}^{n}(W_i - \widetilde{W}_i)^2}{n-s}} \tag{9}$$

where $\widetilde{W}$ is the measured width, W is the predicted width, n is the number of samples, and s is the degrees of freedom in the regression (the number of coefficients in the regression equation).

The average error is used to quantify the bias of the estimate and is defined as:

$$\text{average error} = \frac{\sum_{i=1}^{n}(W_i - \widetilde{W}_i)}{n} \tag{10}$$

The average of the absolute error is used to quantify the average absolute error in real unites of the estimate and is defined as:

$$\text{average absolute error} = \frac{\sum_{i=1}^{n} |W_i - \widetilde{W}_i|}{n} \tag{11}$$

Another metric of model performance used in this analysis is the percent error associated with 90% percentile, meaning that 90% of the predicted widths will be within this error tolerance.

3.3.1 Multiple Regression Model Evaluation

The linear regression results from various combinations of independent variables is discussed in this section to determine the model that does not have high correlation between independent variables, does not include variables with little significance and minimizes the prediction error.

Model 1: $S, D50, Q, H, F$ independent

Linear regression was first performed for all the variables in Eq 4 and the results are shown in Table 14 and Figure 20 in Appendix C. The coefficients for Q and H are significant at greater than a 99% probability. Whereas the coefficients for $D50$ and F and not significant at a 95% probability. Moreover, the coefficient for $D50$ is -0.077 which means that W is only weakly a function of $D50$. However, the value of the $D50$ coefficient is consistent with the results of Parker et al. (2007) and Julien (2002).

In Model 1 (and in all subsequent models) flow is the most dominant variable and has an exponent of greater than 1. This is unusual in the context of downstream geometry relations and most often the exponent of Q is near 0.5. Continuity requires that,

$$Q = VWD \tag{12}$$

where V is the mean channel velocity, D is the flow depth, and the other variables have been previously defined. Variables can also be defined as power functions:

$$W = c_1 Q^{\alpha},\ V = c_2 Q^{\beta},\ D = c_3 Q^{\gamma} \tag{13}$$

Therefore, if α is greater than 1, than one of the other exponents needs to be negative. We do not have the data for velocity, but there is a negative correlation between flow and bank height (D) as shown in Table 5, and based upon a regression analysis, γ is equal to -0.28.

In Model 1, the coefficient for F is positive which is counter to most studies on vegetation and width that find the vegetation presence will tend to narrow channels. Therefore, it is likely that both $D50$ and F are not necessary to include in the regression equation. It does not mean that $D50$ and F are not important in determining width, it only means that given the data in this report, their importance cannot be conclusively determined.

The coefficient for S is significant at more than a 95% probability and is positive as suggested by Leon et al. (2009). The Rio Grande is somewhat unique in that the steeper reaches usually have a wider channel. It is likely due to the relatively high sediment loads on the river as well as the decreasing trend in flow moving downstream.

<u>Model 2: $S, D50, Q, H$ independent</u>

Because F was not considered significant in Model 1, Model 2 includes $S, D50, Q, H$ as independent variables. All variables except $D50$ were significant at a 95% probability. This could be because $D50$ is correlated to both S and H and therefore, one of those variables is likely not necessary.

<u>Model 3: $S, D50, Q$ independent</u>

Previous regression analyses have shown that $S, D50, Q$ are the significant independent variables in predicting downstream channel geometry (e.g., Julien, 2002; Parker, 2007). However, this regression analysis did not show the inverse relationship between W and S that is often reported, rather, we found that increasing slope led to increasing width.

The coefficients of $S, D50, Q$ were significant at the 95% confidence level. The standard error using $S, D50, Q$ as independent variables decreased the error by only 4 ft relative to using only Q as an independent variable.

<u>Model 4: $D50, Q, F$ independent</u>

The coefficients for all the variables were significant at the 95% confidence level, but the exponent for F was positive whereas it was expected to be negative. The error associated with the regression is less than for Model 3, but because the coefficient of F is not physically explainable, we do not recommend using this equation.

Model 5: <u>$D50, Q$ independent</u>

The coefficients for all the variables were significant, but the error using this method was only slightly better than only using Q as a variable.

<u>Model 6: Q, H independent</u>

The R^2 for the regression is only slightly less than that when using all the variables, which suggests that Q and H are the dominant variables when determining the channel width (Table 6). In addition, the standard error of the regression is the same as compared with Model 1. These facts indicate that there is little benefit to including S, $D50$ and F in the regression equation. In fact, because of the multicolinearity between these variables, it could potentially make the predictive capability of the equation worse to include them all.

It should be recognized that H has to be highly correlated to W because river continuity requires that as the width decreases the depth of flow must increase as the result of flow continuity.

Model 7: $D50, S$ independent

The R^2 for this set of independent variables is the lowest of all the models and the error is the highest. This lack of predictive capability of $D50$ and S consistent with the other regression analyses.

Model 8: Q independent

Q was found to have the most correlation with W of any single variable. In fact, including S and $D50$ as independent variables along with Q decreased the standard error by less than 6 ft.

Table 6. Summary of Regression Analysis

Model	Independent Variables	R^2	*Standard error (ft)*	*Average error (ft)*	*Average Absolute error (ft)*	*% error of 90th percentile*
1	*S, D50, Q, H, F*	0.60	101	1.4	70	38
2	*S, D50, Q, H*	0.58	103	1.6	73	38
3	*S, D50, Q*	0.40	121	2.7	89	48
4	*D50, Q, F*	0.44	116	3.1	81	50
5	*D50, Q*	0.38	122	3.2	91	51
6	*Q, H*	0.57	101	1.8	72	39
7	*S, D50*	0.27	133	2.0	100	49
8	*Q*	0.34	125	0.3	94	52

3.3.2 Summary of Results

All the regressions indicate that the dominant variable in predicting *W* is *Q*, the 8-year average of the annual maximum daily average flow. The next most dominant variable is *H*, bank height. The reason why *Q* and *H* are the dominant variables is essentially the requirement of flow continuity. More flow and shorter banks require a wider width to move the water.

Slope (*S*) and median bed material (*D50*) are considered significant, but their inclusion only reduced the standard error in the width by about 4 ft as compared to only including flow in the regression. There may be a benefit to including them when one wants to understand the relative change caused by changing either slope or median bed material. However, there may not be a significant improvement to the accuracy of the prediction especially with standard errors within the range of 100 ft.

Based upon the results above, we do not recommend including vegetation presence (*F*) into the regression. This is not because we believe it is unimportant, but because the limited data and methods used in this analysis do not demonstrate that this variable will improve the predictive accuracy of the regression equation.

Three different regressions are proposed:

$$W = 7.4 \times 10^{-4}\, Q^{1.56}, \qquad \text{std err = 125 ft} \tag{14}$$

$$W = 0.011 Q^{1.37} H^{-0.67}, \qquad \text{std err = 101 ft} \tag{15}$$

$$W = 6.9 Q^{1.1} D50^{-0.12} S^{0.74}, \qquad \text{std err = 121 ft} \tag{16}$$

The reason three different equations are given is that they each could have a separate use. The relationship between *W* and *Q* is useful in that it is the simplest equation and still 90% of the data fall within 50% of the predicted width. The equation with *Q* and *H* gives the least error of all the regressions and demonstrates the importance of bank height on the channel width. However, using *H* in predicting channel width is not entirely predictive because altering *W* can directly change *H*, whereas, for example, changing *W* does not affect *Q*.

The last regression is kept because it demonstrates the effect that *D50* and *S* have on the channel width. It does not necessarily improve the prediction accuracy, but it does help in describing how bed material and slope changes could affect channel width. The application of these equations is discussed in the Design Methodology Section. It is important to remember that Eq. 14, 15, and 16 are empirical regressions developed from data on the Middle Rio Grande between Cochiti and San Marcial for the years 1962, 1972, 1992, 2002, and 2012. Table 6 lists the ranges of reach parameters from the empirical dataset. It is not recommended to apply the equations to cases outside of this range of applicability.

Table 7. Parameter ranges of applicability for Middle Rio Grande width regression equations.

	Minimum	*Maximum*
Width (ft)	155	795
Discharge (cfs)	3,022	5,608
Bank Height (ft)	2.5	10.6
D50 (mm)	0.2	8.7
Slope (ft/ft)	0.0005	0.0013

The above equations were also compared against the Julien (2002) and NRCS (2007) equations and results are found in Table 8. The coefficient of determination (R^2) is substantially lower and the standard error is substantially higher for the Julien (2002) and NRCS (2007) than the proposed equations. The main reason for the worse performance of Julien (2002) and NRCS (2007) is that the flow exponent was only 0.5 whereas the available data showed the width is more sensitive to flow on the Middle Rio Grande. Julien (2002) performed much better than the NRCS (2007) equation, most likely because Julien (2002) included a significantly greater number of sites as part of the regression dataset whereas the NRCS (2007) data originated primarily from the Midwest the Southeast. The predicted versus measured widths for the two methods are given in Appendix C, Figure 34 and Figure 35. The updated regression equations of Lee and Julien (2006) were also evaluated but performed worse for the Rio Grande than Julien (2002).

Table 8. Comparison with Julien (2002) and NRCS (2007) width equations.

Independent Variables	R^2	***Standard error (ft)***	***Average error (ft)***	***% error of 90th percentile***
Q	0.34	125	0.3	52
S, D50, Q	0.40	121	2.7	48
Q, H	0.57	101	1.8	39
Julien (2002)	0.16	143	26	54
NRCS (2007)	0.04	282	-234	316

The potential usefulness of Eq. 14 – 16 is further demonstrated through a design example on the Middle Rio Grande. The Bosque del Apache (BDA) Pilot Channel Realignment Project is currently (2018–2019) being constructed between RM 79–82 near Socorro, NM. Figure 16 (from Holste, 2015) summarizes the channel width values and design methods considered for the river realignment. One-dimensional, mobile bed sediment modeling was then conducted to analyze channel widths of 150, 300, and 450 feet. A final design width of 300 feet was selected, although this was increased in many areas by clearing exotic vegetation adjacent to the main river corridor.

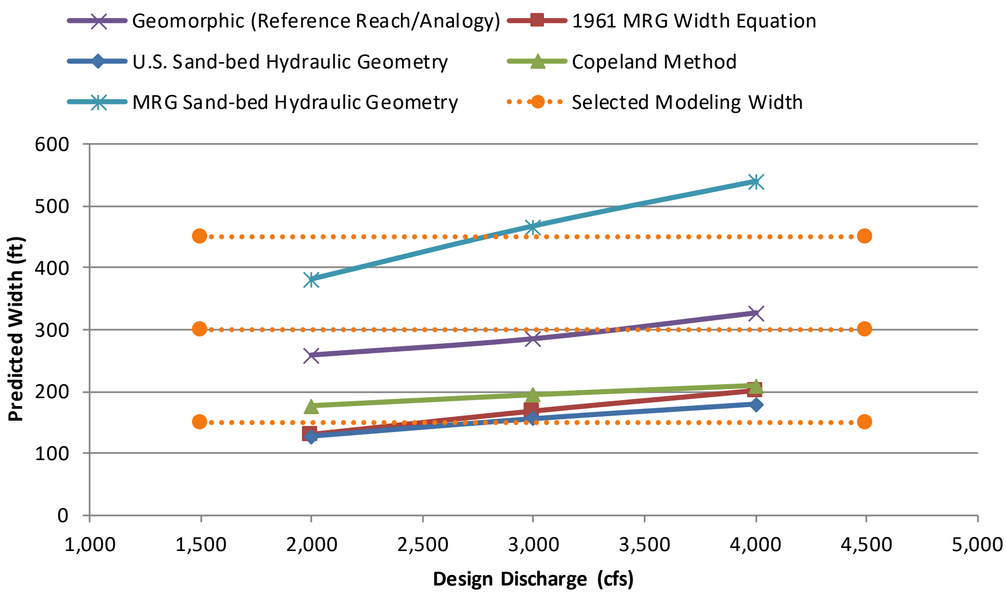

Figure 16. Channel width design values considered for BDA Pilot Realignment Project (Holste, 2015). "MRG Sand-bed Hydraulic Geometry" refers to an at-a-station hydraulic geometry analysis completed by Holste (2015).

Previous width design values are compared to widths calculated from Eq. 14 – 16. Figure 17 plots the calculated channel widths for the realignment project if the current study had been available during design. If the local values of D50 = 0.3 mm and S = 0.0007 are applied, in addition to an assumed bank height of 5 feet, there is not much difference between Eq. 14 – 16. However, as the design bank height is reduced, Eq. 15 predicts larger channel widths. The original design width of 300 feet would be predicted by the following: Eq. 15 assuming a bank height of 3 feet and a discharge of 3,000 cfs, Eq. 15 assuming a bank height of 5 feet and a discharge of 4,000 cfs, Eq. 14 assuming a discharge of 4,000 cfs, or Eq. 16 assuming a discharge of 4,000 cfs. Channel widths greater than the design value are calculated by Eq. 14 – 16 for large discharges and small bank heights. This was accounted for in the design by clearing variable width sections adjacent to the "primary" 300-ft realignment corridor. Most importantly, Figure 17 demonstrates the need for providing freedom and flexibility for a channel to adjust after construction. There is no single "correct" design width due to the inherent variability in water discharge, sediment supply, and other environmental factors.

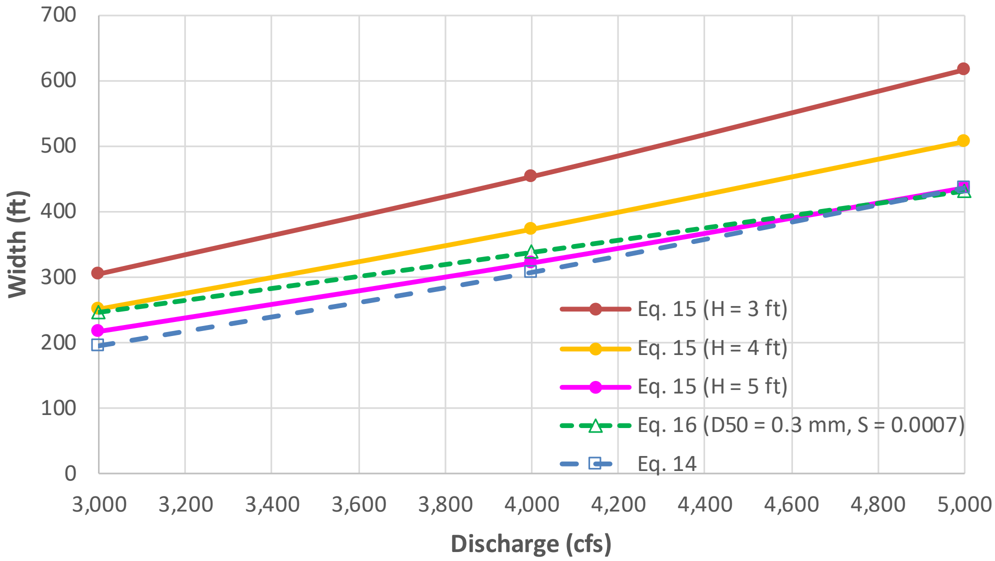

Figure 17. Range of channel widths for BDA Pilot Realignment Project determined by applying Eq. 14–16. Width is most sensitive to the combination of discharge and bank height.

4 At-a-station Geometry

Data from sediment measurements over a range of flows and at multiple locations within the Middle Rio Grande are used to develop a relationship between top width, average depth and flow, meaning to develop at-a-station geometry. Most of the data (301 of 367 data points) are from Reclamation (1961), which means that these channels were likely closer to a pre-disturbance state than the current channels.

The at-a-station relationships will be useful in determining the side slopes of a designed cross section after the total unvegetated width, as determined from the previous regressions, is determined. It is important to note that the width from "at-a-station" geometry is the wetted width as a function of flow at a particular cross section, it is not the unvegetated channel width that is determined from the "downstream geometry" regressions. The suggested method for using both downstream geometry and at-station-geometry relationships is to first predict the unvegetated width from downstream geometry and then adjust the constant in the at-a-station equation so that the at-a-station top width matches the downstream geometry width at the desired design flow rate.

The wetted top width (W) and average channel depth (h) as a function of flow at particular cross sections are given in Figure 18 and Figure 19. We corrected for transformation bias as above following Duan (1983). Here, Q is defined as the instantaneous flow rate. The coefficient and exponent of each of these equations were significant at a 99% confidence level.

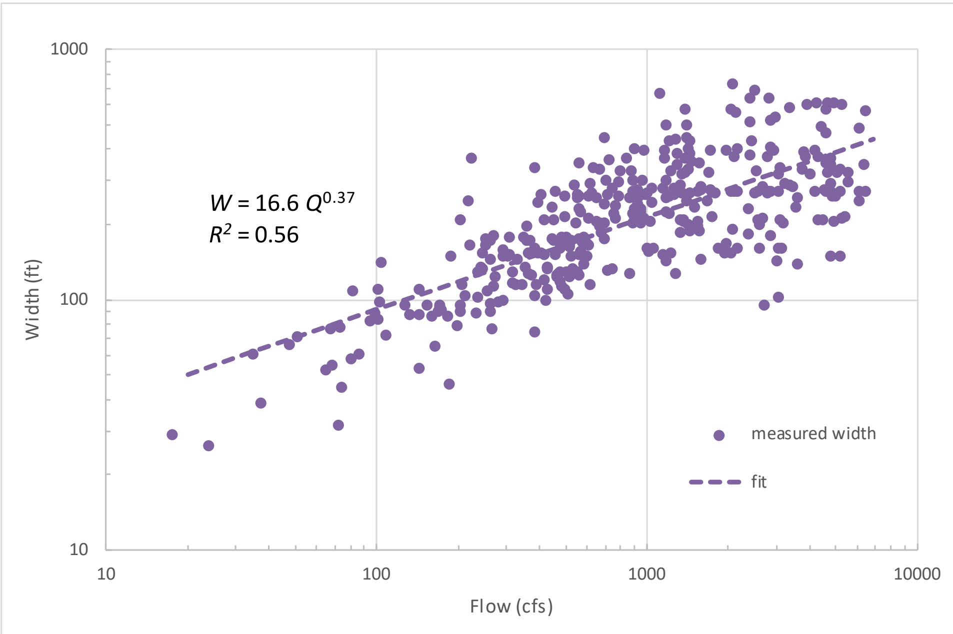

Figure 18. Relationship between flow and wetted top-width at particular cross sections.

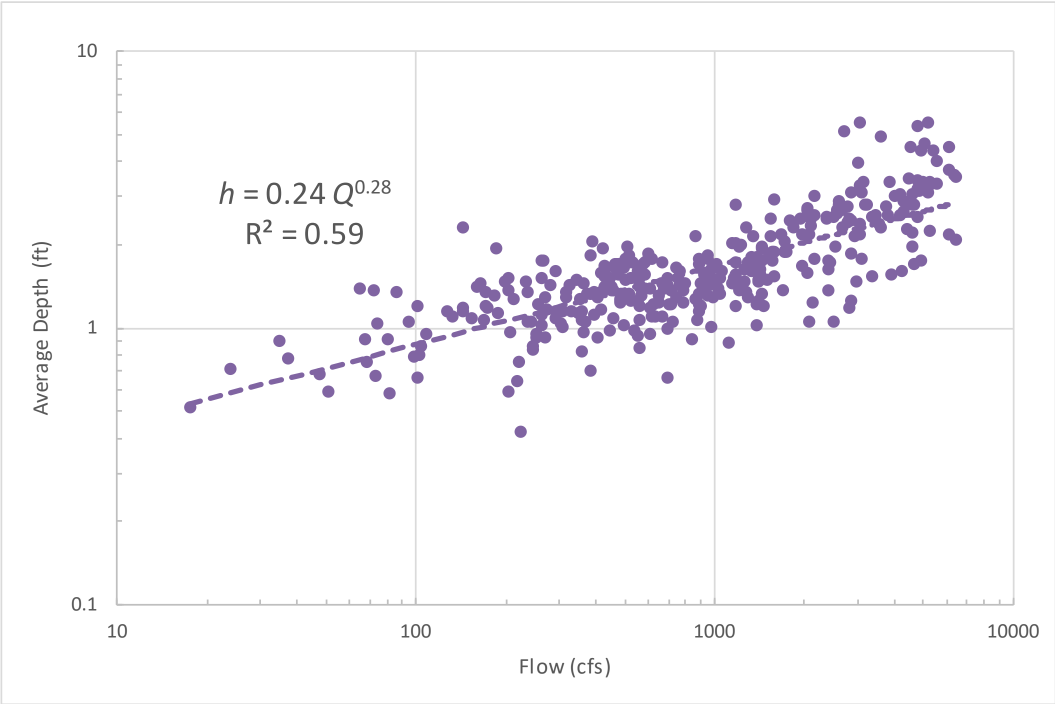

Figure 19. Relationship between flow and average depth at particular cross sections.

5 Design Methodology for Channel Width

This report builds upon the report "Design Width Recommendations" (Baird, 2015), but a simplified design strategy is suggested, and we provide an evaluation of the role of bank height in predicting channel width along with explicit consideration of dynamic widths as mediated by antecedent flood magnitudes. In this section we outline a procedure for channel design utilizing the hydraulic geometry equations we have developed.

There has been a dominant trend of channel narrowing on the Middle Rio Grande; however, the analysis to date does not support a specific threshold for channel width below or above which the river has dramatically different geomorphic behavior.

The following considerations may identify project sites or subreaches that could be considered for application of the proposed design methodology:

- Channel width is less than reach-average width (2012 or more recent data)
- Channel width is significantly less than predicted from Eqs. 14–16
- Rate of channel narrowing is increasing compared to recent and historical rates, or compared to nearby reaches and subreaches

The channel width is assumed to be the width that will be actively influenced by flood flows and cleared of vegetation. This design methodology is **not** intended to generate only single threaded, simple channels. It is recognized that the most biologically valued channels are often complex, multi-width and multi-threaded channels as suggested by Cluer and Thorne (2013). They termed these complex channels "Stage 0" and are thought to be the least disturbed, most biologically valuable stage of channel form existing prior to human disturbance Although Cluer and Thorne (2013) focused on smaller and more heavily forested streams, the concept of biological value from a complex stream morphology still applies. Dean and Schmidt (2011) describe this for the Lower Rio Grande. On the Middle Rio Grande, "Stage 0" likely consisted of a wide, shallow, braided channel that frequently shifted location and migrated across a relatively unvegetated floodplain and with variable width. Flow and sediment changes have drastically altered the channel, but this still provides a valuable conceptual model for habitat conditions favored by native species.

The design methodology does not require that the channel contain the average annual flood (as defined by Q in the regression analysis), and in fact there are habitat benefits when floodplain flow is initiated at discharges smaller than the average annual peak flow. This design methodology also encourages the designer to use multiple channels to accomplish habitat restoration and other goals.

Design Steps

1. Determine *Q*, *D50*, and *S* for the designed reach. The *Q* is uncertain and the designer needs to decide if the channel is intended to be designed for a dry, an average, or or a wet hydrologic scenario. The channel width is expected to not be stable in time as the channel responds to long term wet and dry periods. The average of the maximum annual daily average flow over the preceding eight years may be used as a starting point (as was used in this study), but this value may not be indicative of future flow. In most cases, it is suggested that the slope be similar to the upstream and downstream slopes to maintain sediment continuity. However, there are reasons why slope changes are necessary or desired. For example, the upstream reach could be incised and have a low slope. Designing a wider, steeper channel may be necessary to maintain sediment continuity. The bed material size will be determined by the bed material size of the upstream channel.

2. Determine or design the bank height. The bank height is defined as the elevation when the flow exits the main channel minus the average low flow bed elevation. It is suggested that if restoration of aquatic habitat is a goal of the design, the bank height should be small. This will create more floodplain flow at lower discharges and allow the channel to widen more easily in response to flow. Based upon analysis of historical data, a reasonable range for average bank height is between 2 to 4 feet.

3. Estimate a range of possible top widths of the channel using the 3 regression equations above (Eqs 14–16). In addition, consider the possible error in the equations and design the width appropriately. In restoration projects it may be advisable to under estimate or over-estimate the channel design width depending upon project objectives. For example, if floodplain interaction is a primary goal and a cleared channel is of less concern, then under-designing the channel width may be advisable. Consider designing a multi-threaded river in which the wetted top width is composed of multi-channels. It is also recommended to incorporate width variability into the design, rather than designing a constant width channel.

4. Design the channel side slopes and base width so that it maintains the required average depth at winter base flow. It is recommended that the average depth at the target base flow be approximately 1 foot, but this could be modified based upon other biological criteria. Dudley and Platania (1997) found that Rio Grande silvery minnow most commonly selected depths of 1 – 1.3 feet during the winter. Biologists should be consulted during the design to refine target depth and velocity criteria. The at-station-geometry relationships can also be used in this step to design the channel side slope. Using the unvegetated channel width as computed from Step 3, adjust the constant in the at-a-station equation so that the at-

a-station top width matches the downstream geometry width at the desired design flow rate. This will give a basis for the change in top width with channel depth.

5. Design a variable width rather than a constant width. Soar and Thorne (2001) is an example reference that describes laying out a channel planform with local morphological variability. Their method was developed for meandering channels, so it may be more appropriate for certain reaches of the Middle Rio Grande.

6. Design additional channel and floodplain features such as side channels, point bars, and flood channels as necessary. The methodology for this design is beyond the scope of this report. TSC is currently working on a study with AAO to evaluate the geomorphic performance of various restoration features on the MRG such as embayments, bank lowering, and side channels. Results from this ongoing study will inform design of these additional habitat features.

7. Confirm the design with a 1D flow and sediment transport model to estimate the water surface profiles as well as the long-term erosion and deposition that will occur as a result of the project.

6 References

ASCE (2008). *Sedimentation Engineering*, ASCE Manual and Report on Engineering Practice No. 110, Edited by Garcia, M.H., 1132 pp.

Baird (2015). *Design Width Analysis Recommendations*, prepared for Middle Rio Grande Project, New Mexico, Upper Colorado Region, Report No. SRH-2015-17, Technical Service Center, Denver, CO.

Cluer, B., and Thorne, C. (2013). "A Stream Evolution Model Integrating Habitat and Ecosystem Benefits," *River Research and Applications* (2013), DOI: 10.1002/rra.2631

Culbertson, J.K. and Dawdy, D.R. (1964). A Study of Fluvial Characteristics and Hydraulic Variables, Middle Rio Grande, New Mexico. Geological Survey Water-Supply Paper 1498-F. United States Department of Interior, Geological Survey, United States Government Printing Office, Washington, D.C.

Dean, D.J. and Schmidt, J.C., 2011. The role of feedback mechanisms in historic channel changes of the lower Rio Grande in the Big Bend region. *Geomorphology, 126(3-4)*, pp.333-349.

Doyle, M.W., Shields, D., Boyd, K.F., Skidmore, P.B. and Dominick, D., 2007. Channel-forming discharge selection in river restoration design. Journal of Hydraulic Engineering, 133(7), pp.831-837.

Dudley, R.K. and Platania, S.P. (1997). Habitat Use of Rio Grande Silvery Minnow. Division of Fishes, Museum of Southwestern Biology, Department of Biology, University of New Mexico, Albuquerque, NM.

Duan, Naihua (1983). Smearing Estimate: A Nonparametric Retransformation - Method, *Journal of the American Statistical Association*, Vol., 78, No. 3838. (Sep., 1983), pp. 605-610.

FLO Engineering, Inc. (1995). *Total Sediment Load Calculation for SO Lines, 1993*, Middle Rio Grande Project Hydrographic Data Collection, Delivery Order 0008 Contract No. O-CS-40-08940, prepared for Bureau of Reclamation, Upper Colorado Region, Albuquerque Area Office, Albuquerque, NM.

Holmquist-Johnson, C. and Makar, P. (2006). *2002 Cross Section Geometry Generation and Validation*, prepared for Middle Rio Grande Project, New Mexico, Upper Colorado Region, Technical Service Center, Denver, CO.

Holste (2015). BDANWR Sediment Plug and Habitat Restoration: Design Status Report, Technical Service Center, Denver, CO.

Julien, P. Y. (2002). *River Mechanics*, Cambridge University Press, Cambridge, U.K.

Lagasse, P.F. 1980. An Assessment of the Response of the Rio Grande to Dam Construction – Cochiti to Isleta Reach. Technical Report for U.S. Army Corps of Engineers, Albuquerque District, Albuquerque, New Mexico.

Lee, J-S, Julien, P (2006). "Downstream Hydraulic Geometry of Alluvial Channels," Journal of Hydraulic Engineering, Vol. 132, No. 12, December 1, pp 1347 - 1351.

Leon, C., Julien, P.Y., and Baird, D.C. (2009). “Case Study: Equivalent Widths of the Middle Rio Grande, New Mexico,” *Journal of Hydraulic Engineering*, ASCE, Vol. 135, No. 4.

Makar, P., and AuBuchon, J. (2012). Channel Conditions and Dynamics of the Middle Rio Grande River. Bureau of Reclamation, Technical Service Center, Denver, Colorado, and Upper Colorado Region, Albuquerque Area Office, Albuquerque, New Mexico.

Nordin, C.F. and Beverage, J.P. (1965). Sediment Transport in the Rio Grande, New Mexico. Geological Survey Professional Paper 462-F. United States Department of Interior, Geological Survey, United States Government Printing Office, Washington, D.C.

Nordin, C.F. (1964). Aspects of Flow Resistance and Sediment Transport, Rio Grande near Bernalillo, New Mexico. Geological Survey Water-Supply Paper 1498-H. United States Department of Interior, Geological Survey, United States Government Printing Office, Washington, D.C.

NRCS. (2007). *Alluvial Channel Design*, Part 654 Stream Restoration Design National Engineering Handbook, Chapter 9. United States Department of Agriculture, Natural Resources Conservation Service.

Parker, G., Wilcock, P., Paola, C., Dietrich, W.E., and Pitlick, J. (2007). Physical basis for quasi-universal relations describing bankfull hydraulic geometry of single-thread gravel bed rivers, *Journal of Geophysical Research*, Vol. 112, F04005, doi:10.1029/2006JF000549.

Posner (2017). *Channel Conditions and Dynamics of the Middle Rio Grande (DRAFT)*, Middle Rio Grande Project, New Mexico, Upper Colorado Region.

Reclamation (1961). *Sediment Studies for channelization of the Rio Grande between Cochiti and mouth of Rio Puerco*, Middle Rio Grande Project, New Mexico, Albuquerque Project Office, U.S. Bureau of Reclamation, Department of the Interior, Albuquerque, NM.

Scurlock, D. 1998. From the Rio to the Sierra: An Environmental History of the Middle Rio Grande Basin. General Technical Report RMRS-GTR-5. Fort Collins, Colorado. U.S. Department of Agriculture, Forest Service, Rocky Mountain Research Station.

Sholtes, J.S. and Bledsoe, B.P., 2016. Half-yield discharge: Process-based predictor of bankfull discharge. Journal of Hydraulic Engineering, 142(8), p.04016017.

Singh, V.P., Yang, C.T., and Deng, Z.Q. (2003). Downstream hydraulic geometry relations: 1 Theoretical development, *Water Resources Research*, Vol. 39 (12), 1337, doi:10.1029/2003WR002484.

Soar, P.J. and Thorne, C.R. (2001). *Channel Restoration Design for Meandering Rivers*. Prepared for United States Army Corps of Engineers, Washington, DC.

US Army Corps of Engineers, Waterways Experiment Station, 1998. “SAM Hydraulic Design Package for Channels User’s Manual,” Vicksburg, MS.

Varyu (2013). *2012 Cross Section Geometry Generation and Validation*, prepared for Middle Rio Grande Project, New Mexico, Upper Colorado Region, Report No. SRH-2013-21, Technical Service Center, Denver, CO.

Appendix A. Eliminated Agg/Deg Polygons

Several Agg/Deg locations were not included in the regression analysis because they were determined to not be representative of alluvial channel width on the Middle Rio Grande. The specific locations and the corresponding rationale are listed below.

Agg/Deg	Description
46	Peralta Canyon
97	Galisteo Creek
99	Indian Service Rte. 88 Bridge
139	Borrego Canyon
161	Arroyo de la Vega de Los Tanos
175	Arroyo Tonque
234	Angostura Dam
235	Angostura Dam
236	Angostura Dam
237	Angostura Dam
249	Jemez River
250	Jemez River
299	US 550 Bridge
298	US 550 Bridge
338	Arroyo de la Barranca
357	Arroyo de los Montoya/Harvey Jones Outfall
397	AMAFCA North Diversion Channel Outlet
420	Alameda Bridge
429	Arroyo de las Calabacillas
432	Paseo del Norte Bridge
464	Montaño Road Bridge
494	I-40 Bridge
510	Central Avenue Bridge
529	Bridge Street Bridge
562	Rio Bravo Blvd. Bridge
576	Tijeras Arroyo & AMAFCA South Diversion Channel Outlet
624	I-25 Brdge
654	Isleta Diversion
655	Isleta Diversion
656	Isleta Diversion
657	Isleta Diversion

658	Isleta Diversion
740	NM 6 Bridge
859	NM 309 Bridge
878	Railroad Bridge
948	NM 346 Bridge
965	Abo Arroyo
1054	US 60 Bridge
1099	Salas Arroyo
1127	Arroyo Los Alamos
1160	Large Low Radius Bend
1161	Large Low Radius Bend
1162	Large Low Radius Bend
1163	Large Low Radius Bend
1164	Large Low Radius Bend
1165	Large Low Radius Bend
1166	Large Low Radius Bend
1167	Large Low Radius Bend
1168	Large Low Radius Bend
1169	Large Low Radius Bend
1170	Large Low Radius Bend
1171	Large Low Radius Bend
1172	Large Low Radius Bend
1173	Large Low Radius Bend
1174	Large Low Radius Bend
1175	Large Low Radius Bend
1176	Large Low Radius Bend
1177	Large Low Radius Bend
1178	Large Low Radius Bend
1179	Large Low Radius Bend
1180	Rio Salado
1181	Rio Salado
1182	Rio Salado
1183	Rio Salado
1184	Rio Salado
1185	Rio Salado
1186	San Acacia Constriction and Diversion Dam
1187	San Acacia Constriction and Diversion Dam
1188	San Acacia Constriction and Diversion Dam
1189	San Acacia Constriction and Diversion Dam
1190	San Acacia Constriction and Diversion Dam
1191	San Acacia Constriction and Diversion Dam

1192	San Acacia Constriction and Diversion Dam
1193	San Acacia Constriction and Diversion Dam
1194	San Acacia Constriction and Diversion Dam
1195	San Acacia Constriction and Diversion Dam
1196	San Acacia Constriction and Diversion Dam
1197	San Acacia Constriction and Diversion Dam
1198	San Acacia Constriction and Diversion Dam
1199	San Acacia Constriction and Diversion Dam
1200	San Acacia Constriction and Diversion Dam
1201	San Acacia Constriction and Diversion Dam
1202	San Acacia Constriction and Diversion Dam
1203	San Acacia Constriction and Diversion Dam
1204	San Acacia Constriction and Diversion Dam
1205	San Acacia Constriction and Diversion Dam
1206	San Acacia Constriction and Diversion Dam
1207	San Acacia Constriction and Diversion Dam
1208	San Acacia Constriction and Diversion Dam
1209	San Acacia Constriction and Diversion Dam
1210	San Acacia Constriction and Diversion Dam
1211	San Acacia Constriction and Diversion Dam
1232	San Lorenzo Arroyo
1245	Arroyo de Alamillo
1311	Arroyo de la Parida
1314	Escondida Bridge at Pueblitos Rd.
1330	Nogal Canyon
1338	Arroyo de los Pinos
1359	Arroyo Tinajas/Arroyo de la Presilla
1378	Arroyo del Tajo
1397	Arroyo de las Cañas
1399	Cañas Arroyo
1409	Brown Arroyo/Arroyo Matanza
1445	LFCC Neil Cupp Pump Site
1446	LFCC Neil Cupp Pump Site
1447	LFCC Neil Cupp Pump Site
1448	LFCC Neil Cupp Pump Site
1476	Hwy 380 Bridge
1481	Unnamed Ephemeral Tributary
1511	LFCC North Boundary Pump Site
1513	Check Structure
1606	Eastern Ephemeral Tributary
1643	Eastern Ephemeral Tributary

1703	San Marcial RR Bridge
1685	Straightened Reach
1686	Straightened Reach
1687	Straightened Reach
1688	Straightened Reach
1689	Straightened Reach
1690	Straightened Reach
1691	Straightened Reach
1692	Straightened Reach
1693	Straightened Reach
1694	Straightened Reach
1695	Straightened Reach
1696	Straightened Reach

Appendix B. Reach Averaged Properties

Table 9. Reach Averaged Width (ft)

Reach ID	Width (ft)				
	1962	1972	1992	2002	2012
1	342	294	251	205	248
2	587	580	477	337	311
3	542	554	497	458	440
4	556	521	523	396	371
5	380	414	493	382	290
6	543	612	441	302	220
7	467	223	228	182	192
8	795	567	525	337	279
9	354	196	485	356	313
10	364	207	698	313	239
11	306	178	155	160	146
12	179	128	212	187	177

Table 10. Reach Averaged Slope (ft)

Reach ID	Slope (-)				
	1962	1972	1992	2002	2012
1	0.00125	0.00125	0.00124	0.00121	0.00120
2	0.00095	0.00098	0.00095	0.00091	0.00092
3	0.00093	0.00093	0.00091	0.00091	0.00090
4	0.00082	0.00084	0.00085	0.00082	0.00083
5	0.00071	0.00071	0.00076	0.00072	0.00073
6	0.00073	0.00078	0.00079	0.00073	0.00077
7	0.00089	0.00066	0.00080	0.00066	0.00084
8	0.00093	0.00090	0.00083	0.00084	0.00078
9	0.00072	0.00074	0.00078	0.00075	0.00070
10	0.00075	0.00075	0.00071	0.00067	0.00070
11	0.00066	0.00073	0.00058	0.00051	0.00058
12	0.00068	0.00039	0.00054	0.00054	0.00059

Table 11. Reach Averaged D50 (mm)

Reach ID	D50 (mm)				
	1962	1972	1992	2002	2012
1	0.548	0.548[1]	4.021	8.727	22.000
2	0.445	0.445[1]	1.302	2.036	15.948
3	0.320	0.320[1]	0.555	0.601	4.776
4	0.200	0.200[1]	0.341	0.376	1.759
5	0.200	0.200[1]	0.332	0.338	2.776
6	0.200	0.200[1]	0.304	0.649	2.634
7	0.191	0.191[1]	0.266	0.582	6.269
8	0.191	0.191[1]	0.227	0.388	2.660
9	0.191	0.191[1]	0.231	0.269	0.521
10	0.191	0.191[1]	0.184	0.227	0.312
11	0.170[2]	0.170[2]	0.170	0.201	0.265
12	0.157[2]	0.157[2]	0.157	0.219	0.276

[1] values from 1961 Study
[2] values from 1992 values

Table 12. Reach Averaged Flow (cfs)

Reach ID	8-year Average Annual Maximum Daily Average Flow (cfs)				
	1962	1972	1992	2002	2012
1	5,608	4,713	4,969	3,963	4,033
2	5,427	4,748	4,984	3,902	4,138
3	5,195	4,607	5,020	3,766	3,985
4	5,234	4,618	5,039	3,795	3,987
5	5,269	4,627	5,057	3,822	3,989
6	5,295	4,634	5,069	3,842	3,991
7	5,245	4,563	5,064	3,812	3,971
8	4,916	4,157	5,010	3,610	3,860
9	4,529	3,677	4,945	3,371	3,729
10	4,265	3,350	4,901	3,208	3,640
11	4,000	3,022	4,858	3,045	3,550
12	3,826	2,806	4,829	2,938	3,491

Table 13. Reach Averaged Bank Height (ft)

Reach ID	Bank Height (ft)				
	1962	1972	1992	2002	2012
1	5.8	5.6	6.7	6.7	7.6
2	3.9	2.5	6.3	6.7	7.4
3	3.6	3.3	4.8	4.8	4.6
4	3.6	2.7	3.6	4.1	4.8
5	5.0	2.9	3.8	4.2	6.0
6	5.1	4.0	5.6	4.7	6.4
7	5.9	9.0	10.2	10.6	10.8
8	5.0	5.9	6.7	6.1	5.9
9	4.7	5.9	4.9	3.8	4.1
10	5.1	6.2	3.6	2.8	4.1
11	6.0	7.1	5.7	4.6	7.3
12	7.1	10.7	6.2	4.0	9.4

Appendix C. Regression Results

Table 14. Regression results for Model 1 (Q, S, H, D50, F).

average error	1.4 ft
R2	0.60
standard error	95.1 ft

	Coefficients	*Standard Error*	*t Stat*	*P-value*	*Lower 95%*	*Upper 95%*
ln a	1.969	3.507	0.561	0.577	-5.078	9.016
ln S	**0.655**	**0.270**	**2.428**	**0.019**	0.113	1.197
ln D50	-0.077	0.044	-1.733	0.089	-0.165	0.012
ln Q	**1.102**	**0.260**	**4.237**	**9.9E-05**	0.580	1.625
ln H	**-0.568**	**0.124**	**-4.579**	**3.2E-05**	-0.817	-0.319
F	0.344	0.195	1.758	0.085	-0.049	0.736

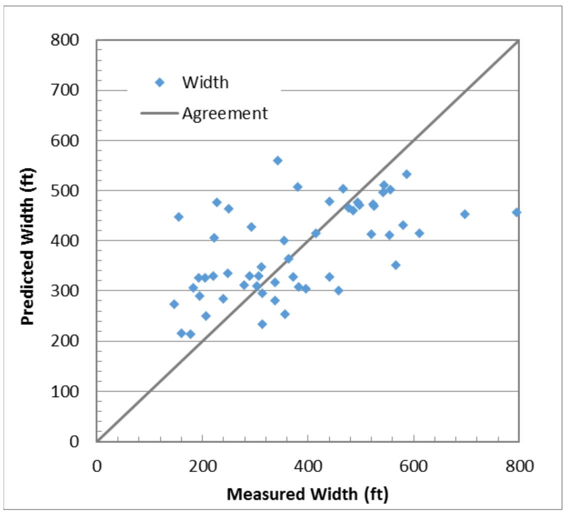

Figure 20. Plot of predicted width versus measured for all variables.

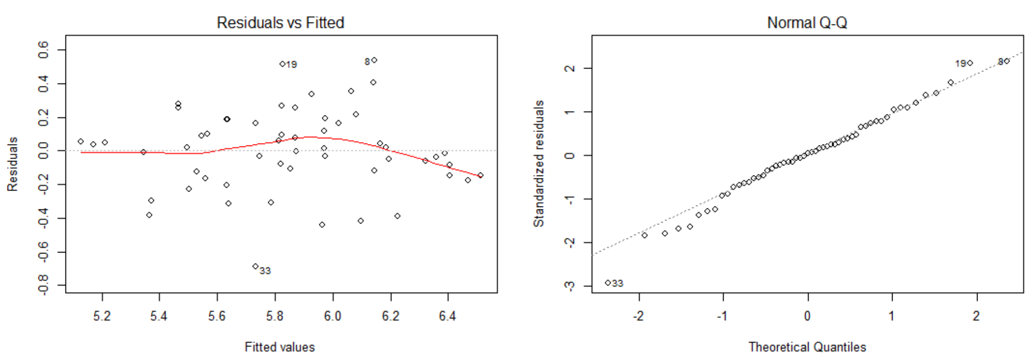

Figure 21. Plot of Residuals for all variables (Q, S, H, D50, F).

Table 15. Regression results for $\ln W = \ln a + b \ln S + c \ln D50 + d \ln Q + e \ln H$.

Average error	1.6
R2	0.58
standard error (ft)	98.0

	Coefficients	*Standard Error*	*t Stat*	*P-value*	*Lower 95%*	*Upper 95%*
ln a	1.300	3.558	0.366	0.716	-5.846	8.447
ln S	0.515	0.263	1.957	0.056	-0.014	1.043
ln D50	-0.037	0.039	-0.953	0.345	-0.115	0.041
ln Q	1.107	0.266	4.168	0.000	0.573	1.640
ln H	-0.653	0.117	-5.594	0.000	-0.887	-0.418

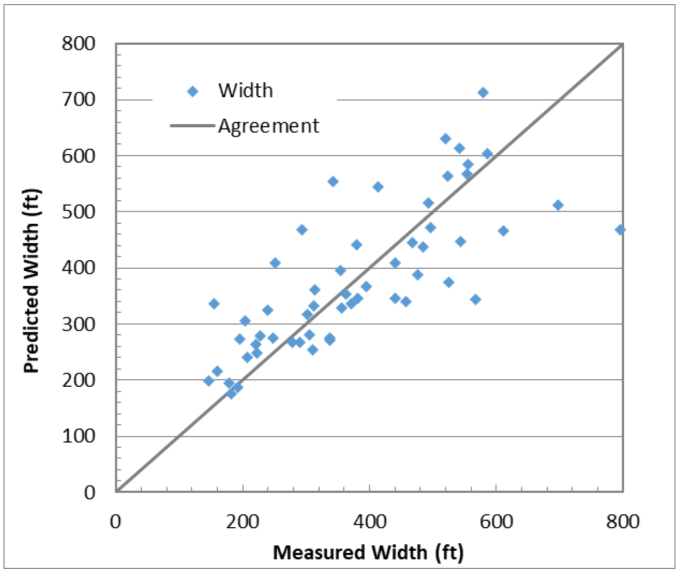

Figure 22. Plot of predicted width versus measured.

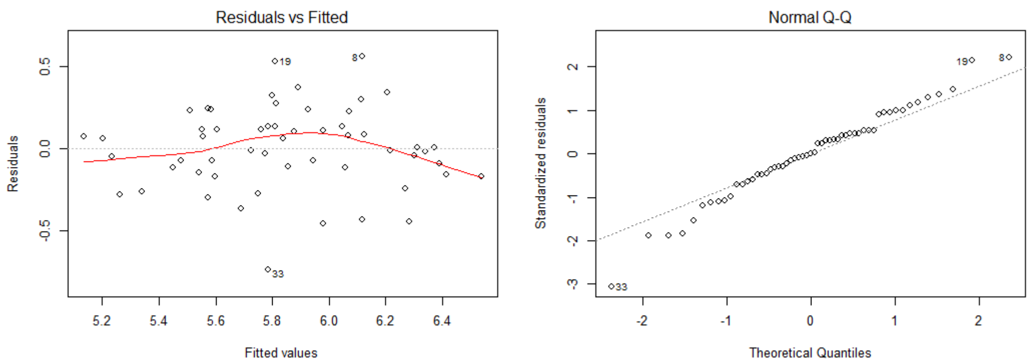

Figure 23. Plot of residuals for $\ln W = \ln a + b \ln S + c \ln D50 + d \ln Q + e \ln H$.

Table 16. Regression results for $\ln W = \ln a + b \ln S + c \ln D50 + d \ln Q$.

average error	2.7
R2	0.40
standard error (ft)	116.6

	Coefficients	*Standard Error*	*t Stat*	*P-value*	*Lower 95%*	*Upper 95%*
ln a	1.871	4.490	0.417	0.679	-7.144	10.886
ln S	0.743	0.328	2.263	0.028	0.084	1.402
ln D50	-0.118	0.045	-2.595	0.012	-0.209	-0.027
ln Q	1.098	0.335	3.275	0.002	0.425	1.771

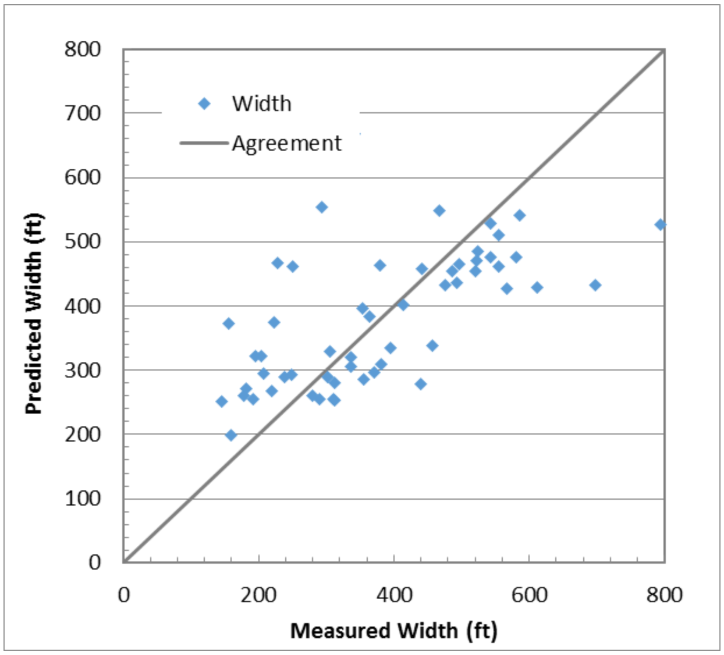

Figure 24. Plot of predicted width versus measured.

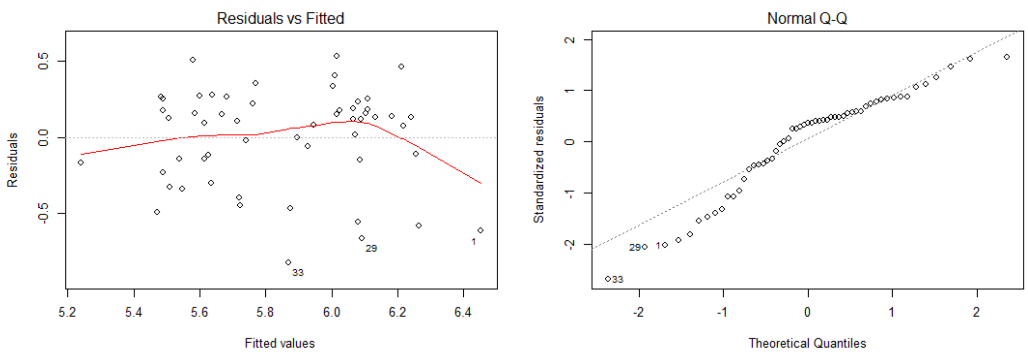

Figure 25. Plot of residuals for $\ln W = \ln a + b \ln S + c \ln D50 + d \ln Q$.

Table 17. Regression results for $\ln W = \ln a + c \ln D50 + d \ln Q + f\, F$.

average error	3.1
R2	0.44
standard error (ft)	111.9

	Coefficients	*Standard Error*	*t Stat*	*P-value*	*Lower 95%*	*Upper 95%*
ln a	-7.858	2.396	-3.280	0.002	-12.667	-3.049
ln S	-0.086	0.038	-2.264	0.028	-0.161	-0.010
ln D50	1.594	0.284	5.614	0.000	1.024	2.164
ln Q	0.543	0.225	2.416	0.019	0.092	0.995

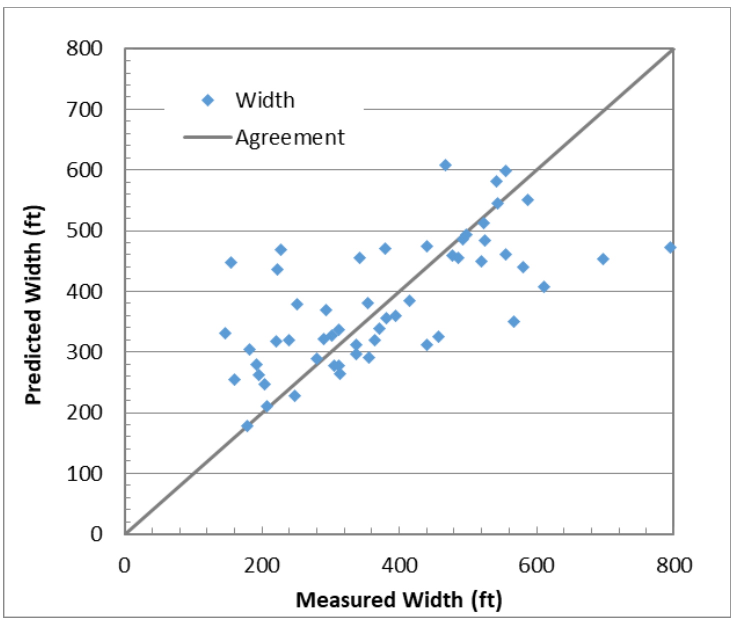

Figure 26. Plot of predicted width versus measured.

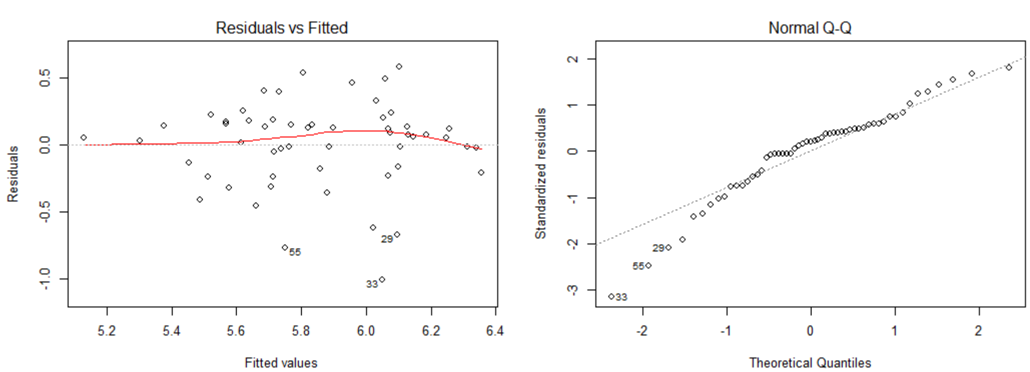

Figure 27. Plot of residuals for $\ln W = \ln a + c \ln D50 + d \ln Q + f\, F$.

Table 18. Regression results for $\ln W = \ln a + d \ln Q + e \ln D50$

average error	3.2
R2	0.38
standard error (ft)	118.5

	Coefficients	*Standard Error*	*t Stat*	*P-value*	*Lower 95%*	*Upper 95%*
ln a	-6.765	2.459	-2.751	0.008	-11.700	-1.830
ln Q	-0.054	0.037	-1.466	0.149	-0.129	0.020
ln D50	1.504	0.294	5.109	0.000	0.913	2.094

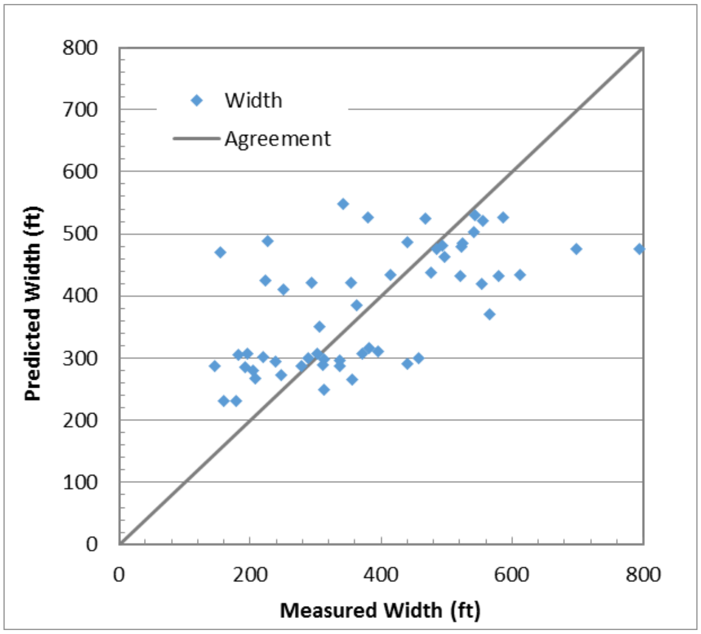

Figure 28. Plot of predicted width versus measured.

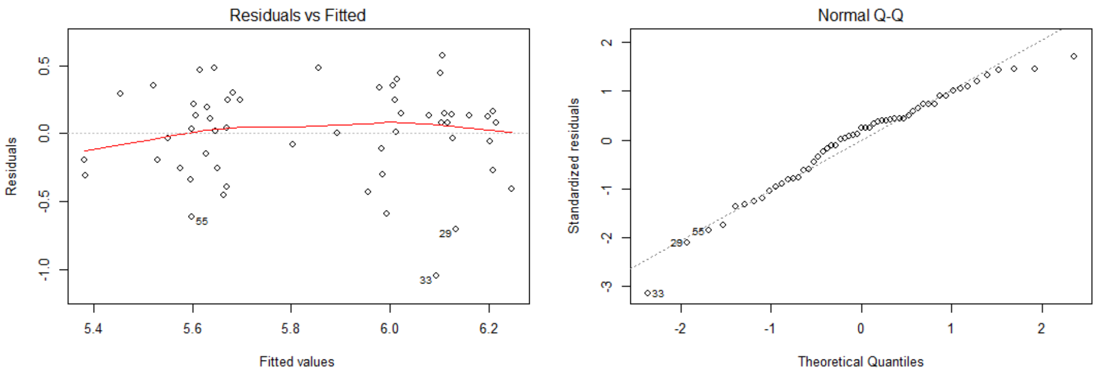

Figure 29. Plot of residuals for $\ln W = \ln a + c \ln D50 + d \ln Q$.

Table 19. Regression results for $\ln W = \ln a + d \ln Q + e \ln H$

average error	1.8
R2	0.57
standard error (ft)	98.4

	Coefficients	*Standard Error*	*t Stat*	*P-value*	*Lower 95%*	*Upper 95%*
ln a	-4.544	1.944	-2.337	0.023	-8.445	-0.642
ln Q	1.374	0.228	6.016	0.000	0.916	1.833
ln H	-0.674	0.110	-6.148	0.000	-0.894	-0.454

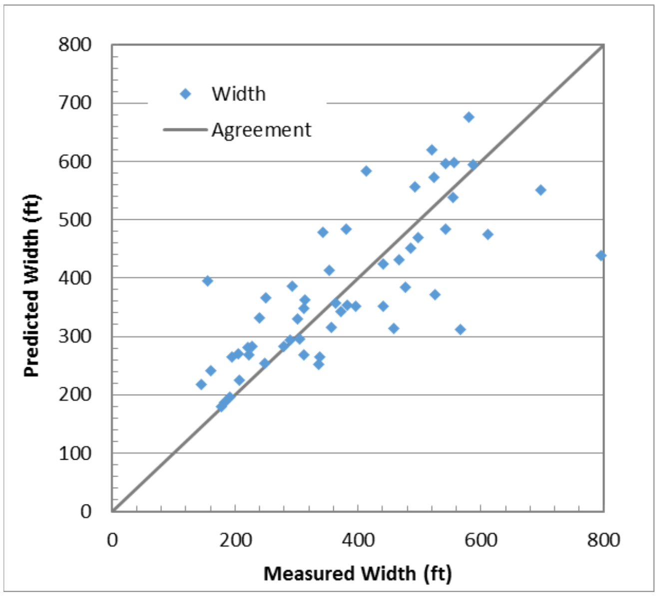

Figure 30. Plot of predicted width versus measured.

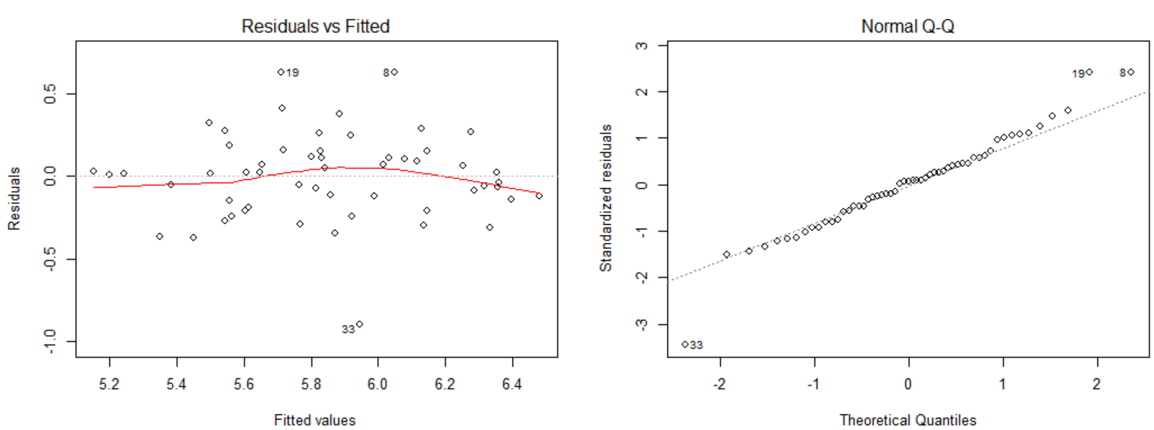

Figure 31. Plot of residuals for $\ln W = \ln a + d \ln Q + e \ln H$.

Table 20. Regression results for $\ln W = \ln a + d \ln Q$

average error	2.6
R2	0.34
standard error	122.2

	Coefficients	*Standard Error*	*t Stat*	*P-value*	*Lower 95%*	*Upper 95%*
ln a	-7.215	2.466	-2.925	0.005	-12.162	-2.268
ln Q	1.562	0.295	5.300	0.000	0.971	2.153

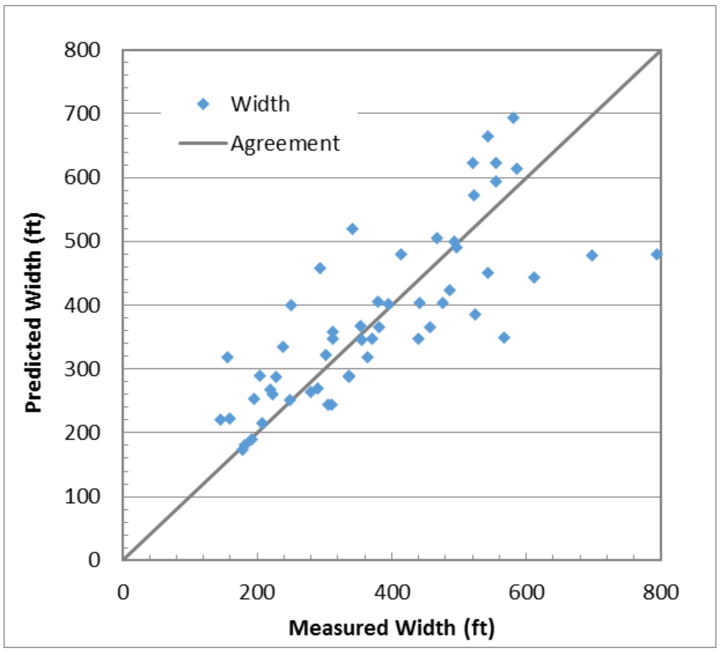

Figure 32. Plot of predicted width versus measured for $\ln W = \ln a + d \ln Q$.

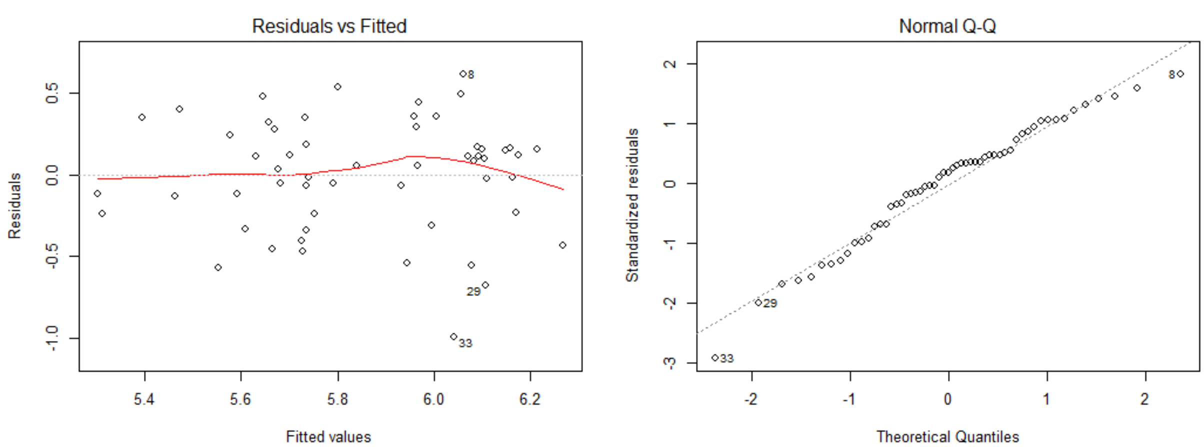

Figure 33. Plot of residuals for $\ln W = \ln a + d \ln Q$.

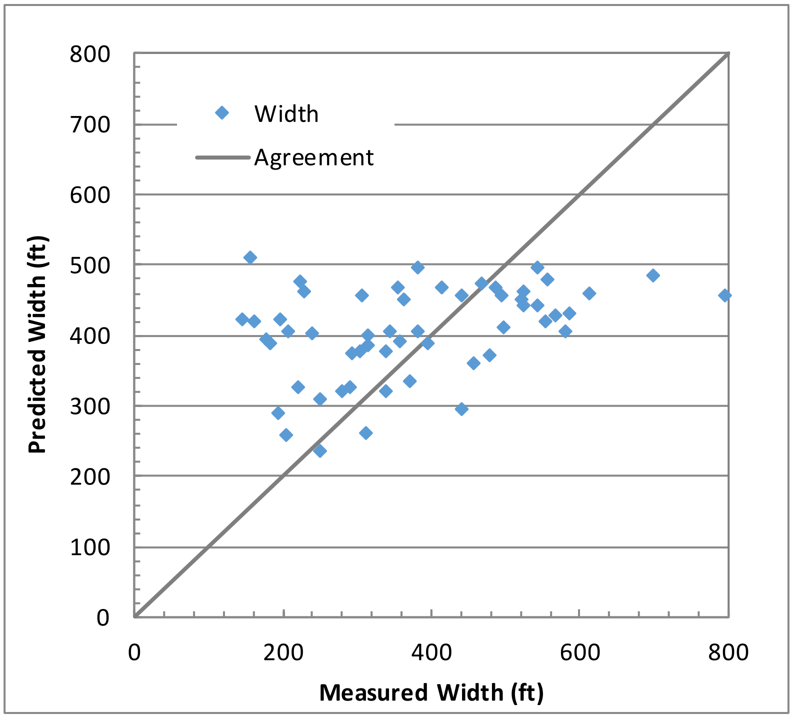

Figure 34. Plot of predicted width versus measured for Julien (2002) regression equation.

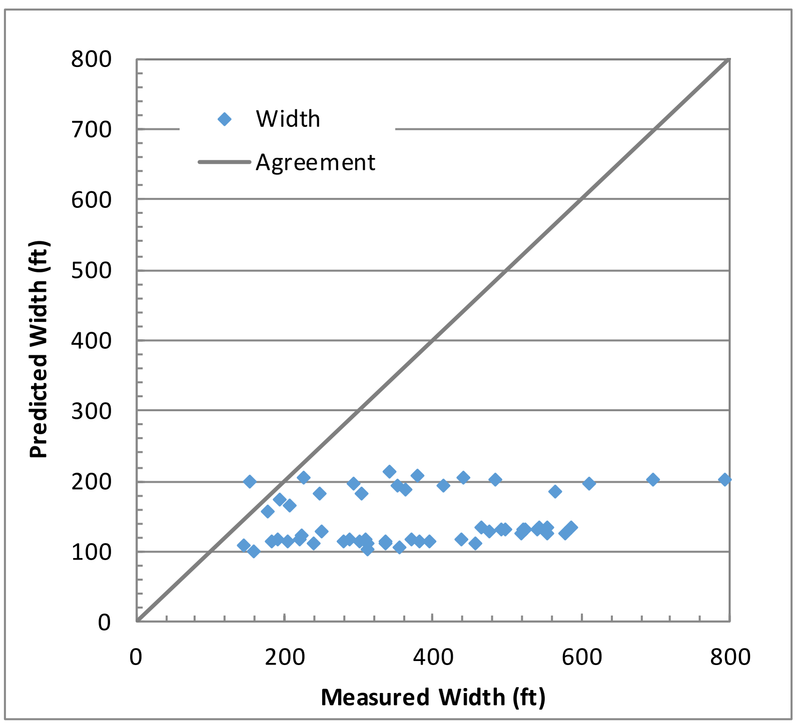

Figure 35. Plot of predicted width versus measured for NRCS (2007) regression equation